AN ANALYSIS OF THE CONTINUOUS REMOVAL OF LIQUIDS FROM GAS WELLS

------------- * -------------

A THESIS
PRESENTED TO
THE FACULTY OF THE
CULLEN COLLEGE OF ENGINEERING
UNIVERSITY OF HOUSTON
HOUSTON, TEXAS

IN PARTIAL FULFILLMENT
OF THE REQUIREMENTS FOR THE DEGREE
MASTER OF SCIENCE IN PETROLEUM ENGINEERING

BY

RONALD G. TURNER

AUGUST 1967

ACKNOWLEDGEMENT

The author wishes to acknowledge the assistance and guidance offered by Dr. M. G. Hubbard in the preparation of this report. The contribution of Dr. A. E. Dukler, whose suggestions were invaluable, is also acknowledged. Special appreciation is expressed to Mr. Ovid Baker and Mobil Oil Company for their interest and contribution of field data, and to Pan American Petroleum Corporation and Humble Oil and Refining Company for their cooperation in the acquisition of data. Grateful appreciation is extended to Baker Oil Tools, Inc. for permission to complete and publish this work, and to Mrs. Betty Nixon and Mrs. Deloris Kuykendall who typed the manuscript. Also to the author's wife, Paula, without whose patience and understanding this work would have been impossible, a special debt of gratitude is owed.

AN ANALYSIS OF THE CONTINUOUS REMOVAL OF LIQUIDS FROM GAS WELLS

*

AN ABSTRACT OF
A THESIS
PRESENTED TO
THE FACULTY OF THE
CULLEN COLLEGE OF ENGINEERING
UNIVERSITY OF HOUSTON
HOUSTON, TEXAS

IN PARTIAL FULFILLMENT
OF THE REQUIREMENTS FOR THE DEGREE
MASTER OF SCIENCE IN PETROLEUM ENGINEERING

BY

RONALD G. TURNER

AUGUST 1967

ABSTRACT

Natural gas wells producing liquid phase material along with the gas must be flowed at a gas rate sufficient to continuously remove the liquids. Otherwise these liquids will accumulate in the wellbore, restricting the flow of gas and affecting the calculations associated with standard performance tests required by most states. The minimum gas flow rate necessary to prevent accumulation is therefore significantly important to gas producers.

The purpose of this thesis is to analyze the methods of liquid mass transport in a two-phase gas/liquid system flowing co-currently upward, and to establish a method of calculating the minimum gas flow rate that will carry the liquid phase material continuously up the conduit.

The mass transport mechanisms in vertical tubes are developed theoretically with continuous upward moving annular liquid films, flooding countercurrent annular films and entrained liquid drop movement each treated separately. The minimum gas flow conditions for each mechanism are derived and the developments tested against field flow test data. A method of predicting the minimum gas flow rate necessary to continuously remove liquids from gas wells is presented.

TABLE OF CONTENTS

LIST OF TABLES

Chapter I

INTRODUCTION

Naturally occurring gas phase hydrocarbons have been produced from wells as a by-product of liquid oil production for many years. Prior to the construction of pipeline networks linking the population centers of the East to the Gulf Coast, no significant market existed for this natural gas. The gas produced was a nuisance and in most cases it was flared. In recent years, however, a large domestic market has developed for gas phase hydrocarbons, both as fuel and as a raw material for petrochemical products. Gas wells, those wells that produce essentially gas phase material from the reservoir, have since become economically attractive. Due to the inherent low density of natural gas, which is predominately methane, gas wells have a low pressure gradient and large volumes can be produced by natural expansion from the reservoir, with only moderate pressure drop.

In a great many wells, there are liquid phase components associated with the gas. The liquid may be either water or hydrocarbon or both, and the origin may be the interstitial space in the reservoir matrix and/or condensation during transport to the surface. This liquid phase must be removed from the wellbore or it will collect in the bottom and develop an additional hydrostatic back pressure on the formation that will restrict the flow of gas into the well. If the reservoir pressure is insufficient to overcome this additional back pressure, the well will cease to flow. Under these circumstances, the well will require artificial means, such as a mechanical pump to remove the liquid.

In wells with reservoir pressures high enough to resist cessation of flow due to liquid accumulation, the liquids, if not removed on a steady state continuous basis, will be ejected intermittently as slugs. This "choking" or "loading up" condition results in distortion of the bottom hole pressure calculations performed in routine flow tests required for regulatory purposes in most states. Smith (22) states, "The accumulation of liquid in the wellbore is probably the most serious cause of erroneously calculated bottom hole pressure." The lack of continuous removal of these liquids will also yield erroneous gas/liquid ratios.

The determination of the minimum gas flow rate, below which accumulation and subsequent choking or loading up will take place, has been the object of several investigations. Vitter (24), Duggan (3) and Flaitz, etal (6) each suggested minimum average gas phase velocities necessary to remove liquids from gas wells. These were based on field experience. Jones (15) and Dukler (5) derived equations based on physical properties and flow geometry to predict the minimum flow rate.

This thesis is an analysis of the possible natural transport mechanisms available to carry liquids out of gas wells, and the development of a method for calculating the minimum flow rate necessary to continuously remove these liquids. Two possible methods of movement, i.e., film movement along the walls and drop movement in the gas stream are treated analytically to determine the limiting gas flow rate for continuous liquid transport in vertical conduits and the resulting correlations tested against field tests and laboratory data.

Chapter II

PRIOR INVESTIGATIONS

Several authors (3, 15, 20, 22, 24) have mentioned the problems that can be associated with inadequate gas flow rates and subsequent gas flow restriction due to liquid accumulation during well tests. Of the tests that are performed on gas wells, the split stream test and the multi-rate back pressure test are the most common.

The split stream test, designed to measure gas/liquid ratios, is accomplished by introducing a small diameter probe into the gas stream at the wellhead and removing a local sample which is then processed through phase separation and analysis equipment. In order to obtain accurate gas/liquid ratio measurements by this method, it is necessary for the liquid phase to be uniformly distributed throughout the production stream such that the probe samples a proportionate amount of each phase. Flaitz and Parks (6) suggested that an average gas velocity at the wellhead of 15-20 ft per second was adequate to insure entrainment of sufficient liquid phase in the center of the gas stream to give representative gas/liquid ratios in a split stream test. This figure was obtained empirically from field tests of many wells.

The back pressure test is the most common test performed on gas wells and is standardized throughout most of the United States. The basis for this test is the gas well deliverability equation obtained from Darcy's law for the steady state radial flow of gas into a wellbore (2),

$$Q = C(P_F^2 - P_S^2)^n$$

where Q = Gas flow rate

P_F = The shut-in bottom hole formation pressure

P_S = The flowing bottom hole sandface pressure

n = A constant whose value is a function of reservoir and fluid properties

C = A constant whose value is a function of reservoir and fluid properties

An analysis of this equation indicates that a plot of the difference in the squares of the shut-in and flowing bottom hole pressure, $(P_F^2 - P_S^2)$, versus flow rate, Q, on log-log paper should yield a straight line of slope n. Once determined, this straight line can be used to predict the gas well performance under any formation back pressure. The determination of this straight line from field flow tests is the purpose of back pressure testing. (See Fig. 1)

The bottom hole flowing pressure (P_S) is generally calculated from the surface pressure observed during the test. The calculation of bottom hole flowing pressure has been explored in detail by Roxburgh (21). The methods generally employed in calculating bottom hole flow pressure involve the determination of the combined effects of the pressure head due to the weight of the gas column and the frictional pressure drop resulting from flow. The accumulation of a liquid column in the bottom of the well, a condition known as "loading up", will not only create a changing (unsteady) pressure condition at the bottom, but also the presence of the added hydro-

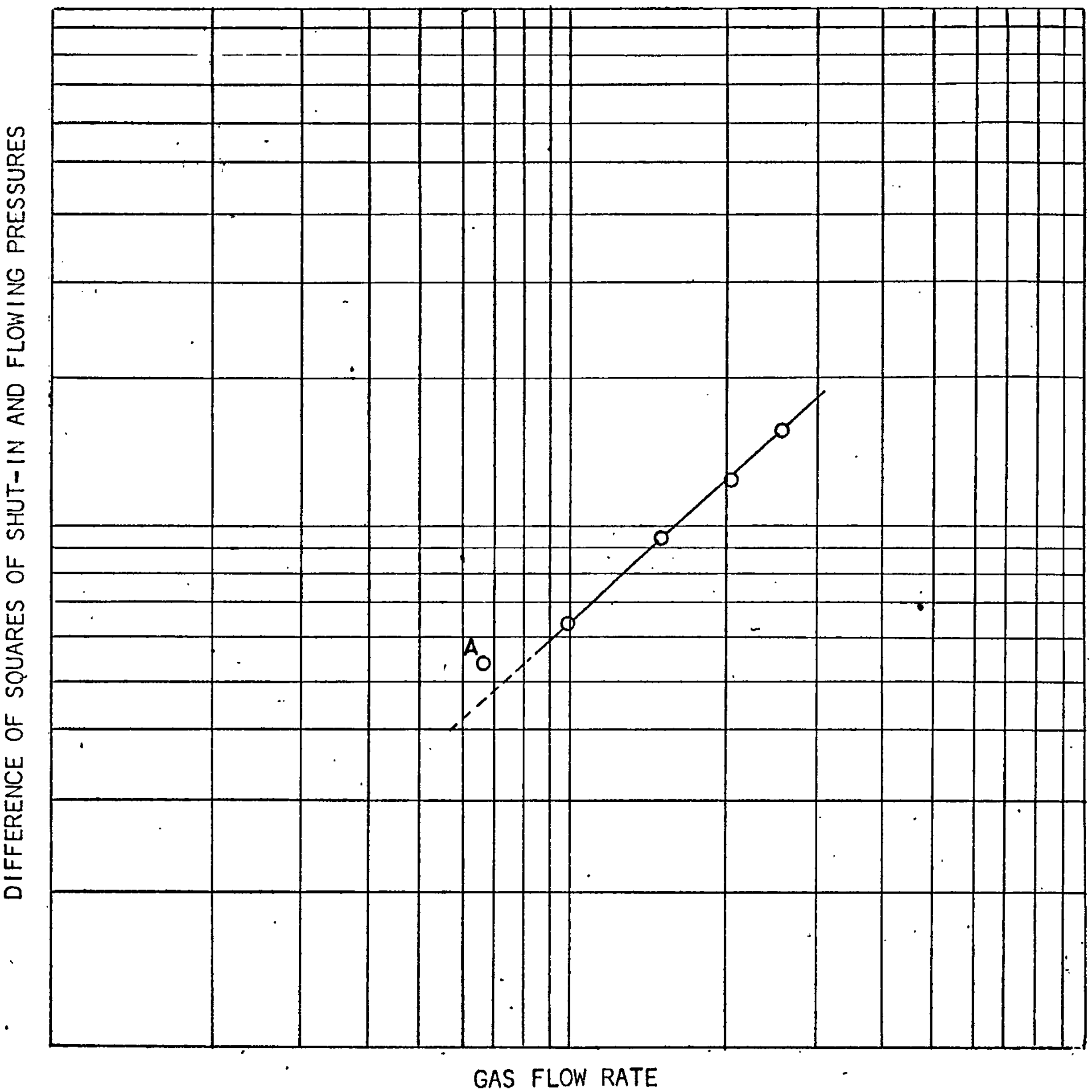

Figure I

Typical Back Pressure Test Curve

static back pressure on the formation, due to the liquid column weight, will reduce the gas flow rate below that which would exist were this added back pressure not present. This results in the calculation of a bottom hole pressure which is lower than the actual value (Fig. II).

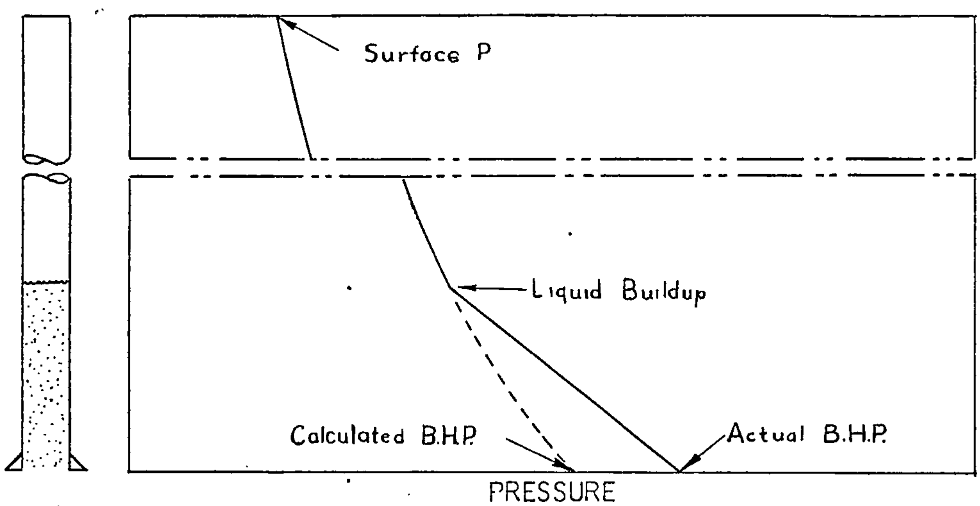

Figure II

Typical Pressure Gradient

The liquid column height is unknown and the inclusion of it in the calculation procedure is impossible. Using the erroneously calculated lower bottom hole pressure for P_s results in a larger value in for the quantity $(P_F^2 - P_s^2)$, which displaces the data point from the characteristic straight line back pressure test curve as shown with Point "A" in Fig. I. The back pressure test, therefore, requires that steady state flow conditions exist in the conduit, and that all liquid entering the wellbore must be removed continuously. The accumulation of liquid in the production conduit will result in a "loaded up" condition and an erroneous back pressure test curve.

Rawlins and Schellhardt (20) tested several "wet" gas wells and reported the effect of liquid buildup on pressure calculations as well as the flow rate necessary in each test to keep liquids from accumulating. No derivation of a method for calculating this flow rate was attempted however. Vitter (24) suggested that flowing wellhead gas velocities of 6 to 10 feet per second would be sufficient to remove liquids during back pressure testing. This was based on field observation. Duggan (3) concluded that, for gas condensate wells which are not producing water, a flowing wellhead gas velocity of 5 feet per second was sufficient for liquid removal. This study included tubing and annular configurations on wells with wellhead pressures from 1100 to 8000 psi. Duggan based his determination of well "load up" on the appearance of the back pressure curve, i.e., if a point at a low rate varied from the straight line by showing a higher value for the difference of the squares of the pressures (See Fig. I, Point A), the well was accumulating liquids while flowing at this test rate.

The above mentioned velocities were obtained through field testing and were meant to be general rules of thumb for field use. The first analytical approach to calculation of a flow rate satisfactory for liquid removal was taken by Jones (15).

The equation which Jones suggests is the result of a theoretical treatment adjusted on the basis of field results. The original development by Jones is not published, but was based on the assumption that the liquid would be in the form of drops and that if the largest of these drops were removed, all drops would be. Jones reasoned that the largest drop size that can exist in a string of tubing would be one having a diameter equal to the inside diameter of the tubing. This development gave a grouping of parameters which for application to field problems required information from the individual wells. This was the first approach that included individual well parameters in the determination of the minimum flow rate necessary to unload liquids. A derivation of Jones' equation is presented in Appendix B. The final result is

$$Q_J = D^{\frac{5}{2}}\left(\frac{P}{MTZ}\right)^{\frac{1}{2}}$$

where Q_J = Flow rate MMCF/Day

D = Diameter (inside) of tubing (in)

P = Absolute bottom hole pressure (psia)

M = Molecular weight of gas (lbs/lb mole)

T = Absolute bottom hole temperature (°R)

Z = Compressibility factor (at P & T)

This equation yields conservative flow rates, i.e., higher flow rates than the actual required minimum.

Dukler presented an unpublished paper at the American Petroleum Institute Meeting in Albuquerque, New Mexico in 1961 in which he concluded that the actual behavior of the liquid phase involved both

both drop activity in the gas core and liquid film activity at the surface of the conduit. He then developed a drop model and suggested a film model to predict this behavior. (These models are presented and an extension proposed in Chapter III)

Chapter III

TRANSPORT MECHANISMS

The Continuous Film Model

Liquid phase accumulation on the walls of a conduit during two-phase gas/liquid flow is inevitable due to the impingement of entrained liquid drops and the condensation of vapors. The movement of the liquid on the wall is therefore of interest in the analysis of liquid removal from gas wells. If the annular liquid film must be moved upward along the walls in order to keep a gas well from loading up, then the minimum gas flow rate necessary to accomplish this is of primary interest.

The co-current vertical upward flow of gas core-liquid film systems has been studied in several laboratory investigations and its theoretical understanding (1,4,9) has advanced to a point where mathematical modeling is possible. The approach presented here is after Hewitt (9) and his treatment of the Dukler (4) analysis. (A full mathematical development is found in Appendix C.)

In an annular liquid film of thickness m on the walls of a vertical tube, the transport in the upward direction is a result of the interfacial shear, τ_i, of the moving gas on the surface of the liquid (Fig. III). This motion is resisted by the action of gravity and wall

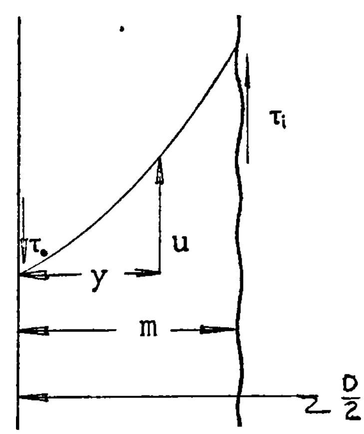

Figure III

Upward Moving Liquid Film

friction. At any point y distance from the wall there exists a velocity u and a shear stress τ. The resisting shear stress at the wall is τ_o. A steady state force balance shows that a any point y

$$\frac{\tau}{\tau_o} = 1 + \frac{y \rho_L g_L}{\tau_o g_c} \qquad 3.01$$

In dimensionless form, Eq. 3.01 becomes

$$\frac{\tau}{\tau_o} = 1 + y^+ \frac{\sigma^3}{\eta} \qquad 3.02$$

Where

σ is defined by Eq. 15, Appendix B.

$$y^+ = \frac{u^* y \rho_L}{\mu_L}$$

$$u^* = \sqrt{\frac{\tau_o g_c}{\rho_L}}$$

$$u^+ = \frac{u}{u^*}$$

$$\eta = \frac{m\, u^* \rho_L}{\mu_L}$$ (the dimensionless film thickness)

Eq. 3.02 is the shear stress distribution as a function of the distance from the wall of the tube. The Gill and Scher (7) momentum transport hypothesis yields the relationship

$$\frac{\tau}{\tau_o} = \left[1 + k^2 y^{+2} \left(1 - e^{-\phi \frac{y^+}{y_m^+}} \right)^2 \frac{du^+}{dy^+} \right] \frac{du^+}{dy^+} \qquad 3.03$$

where

$$y_m^+ = \frac{u^* D \rho_L}{2 \mu_L}$$

$$\phi = \frac{y_m^+ - 60}{22}$$

$$k = .36$$

Eq. 3.03 is the shear stress distribution as a function of the velocity gradient and the distance from the wall. The velocity distribution as a function of the distance from the wall may be found by equating 3.02 and 3.03 and solving explicity for u^+.

$$u^+ = \int_0^{y^+} \frac{2\left(1 + y^+ \frac{\sigma^3}{\eta}\right)}{1 + \sqrt{1 + 4k^2 y^{+2}\left(1 - e^{-\phi \frac{y^+}{y_m^+}}\right)^2 \left(1 + y^+ \frac{\sigma^3}{\eta}\right)}}\, dy^+ \qquad 3.04$$

Eq. 3.04 is the dimensionless velocity distritution in the film. The liquid phase flow rate is obtained from the equation

$$W_L = \pi D \mu_L \int_0^{\eta} u^+ dy^+ \qquad 3.05$$

Eq. 3.04 and 3.05 may be used to evaluate the minimum gas flow rate required to move the film steadily upward. For this application it is necessary to establish the relationship between the shear stresses and the gravitational forces in the film at the minimum condition of upward flow. Since the interfacial shear, τ_i, provides the motivating force for moving the film upward and the gravitational "shear stress", $\frac{m \rho_L g_L}{g_c}$, and the shear stress at the wall, τ_o, are resisting movement, the minimum flow condition for film movement will be when the interfacial shear, τ_i, approaches the value of the gravitational "shear" and the shear stress at the wall, τ_o, approaches zero.

The ratio $\frac{m \rho_L g_L/g_c}{\tau_i} = X$ approaches 1.0 (i.e., the gravitational shear stress equals the interfacial shear stress) at the limiting condition. For the purpose of analysis, X must be slightly less than one (i.e., the interfacial shear must be larger than the gravitational shear stress, and τ_o must be greater than zero). Hewitt (9) suggests that .99 is the maximum practical value of X.

Assuming that X = .99 at the minimum gas flow rate condition, it is possible to evaluate the necessary parameters to integrate Eq. 3.04 and 3.05. The relationships utilized are

$$\sigma^3 = \frac{X}{1 - X}$$

$$\frac{\beta}{\eta^{2/3}} = \frac{1}{X^{2/3}(1 - X)^{2/3}}$$

where

$$\beta = \frac{F\ D\ \rho_L^{2/3} g_L^{1/3}}{4\mu^{2/3}}$$

$$F = \frac{\frac{\Delta P}{\Delta X} - \rho_G \frac{g_L}{g_c}}{\rho_L \frac{g_L}{g_c}}$$

$$\left[\frac{\Delta P}{\Delta X} - \rho_G \frac{g_L}{g_c}\right] = \text{the two phase pressure drop} = \frac{\Delta P}{\Delta X_{TP}}$$

A modification of the Martinelli (17) two phase pressure drop correlation is employed to evaluate the $\frac{\Delta P}{\Delta X_{TP}}$. The relationship used is

$$\Phi_G = 3.3 \quad \chi^{.22}$$

The terms Φ_G and χ are the original Martinelli groupings

$$\Phi_G = \sqrt{\frac{\frac{\Delta P}{\Delta X_{TP}}}{\frac{\Delta P}{\Delta X_G}}}\ .$$

and

$$X = \sqrt{\frac{\frac{\Delta P}{\Delta x_L}}{\frac{\Delta P}{\Delta x_G}}}$$

The calculation procedure to test the development against field flow tests involves trial and error. The steps are:

1. Fix the liquid phase flow rate (the producing liquid rate during the field test).
2. Assume a gas flow rate and calculate the parameters σ^3 and η.
3. Numerically integrate Eq. 3.04 to obtain values of u^+ as a function of y^+.
4. Use these values to numerically integrate Eq. 3.05 to obtain a calculated liquid flow rate.
5. The calculated liquid flow rate is compared to the known flow rate from Step 1, and the gas rate adjusted for an iterative loop.
6. The iteration is carried to convergence of the known and calculated liquid flow rates. The adjusted gas flow rate that leads to a calculated liquid flow rate that is the same as the known value is the minimum gas flow rate necessary to move a liquid film steadily upward.
7. This gas flow rate can then be compared to the gas flow rate derived during the field test.

The Flooding Film Model

In the analysis of continuous upward film movement, the minimum gas flow rate to support such upward movement was the point of investigation. Reduction of the gas flow rate below this point would result in an unstable condition resulting in churning and slugging. A similar condition of instability can occur in a system that initially involves a film moving counter-current to the gas stream. This condition, known as "flooding", is the point in counter-current liquid film/gas core flow when the gas and liquid flow rates are such that the film becomes disturbed to such a state that liquid phase is carried in the direction of the gas. This condition is similar to that developed in the continuous film model, except that the liquid is initially flowing in the opposite direction. Direct mathematical analysis is not yet possible, however, an excellent empirical method is available.

The calculation of the "flooding point" in a gas well is directed toward finding the minimum gas flow rate that will reverse a film just as it starts to move counter-current to the gas flow. This will insure that no film will reach the bottom where accumulation can occur.

Wallis (9, 25) suggested the following empirical correlation for calculating the flooding point in tubes.

$$\overset{*}{V}_L^{\frac{1}{2}} + \overset{*}{V}_G^{\frac{1}{2}} = C \qquad 3.06$$

where

$$\overset{*}{V}_L = V_{SL} \ \rho_L^{\frac{1}{2}} \left[g_L D \ (\rho_L - \rho_G) \right]^{-\frac{1}{2}} \qquad 3.07$$

$$\overset{*}{V}_G = V_{SG} \ \rho_G^{\frac{1}{2}} \left[g_L D \ (\rho_L - \rho_G) \right]^{-\frac{1}{2}} \qquad 3.08$$

C = 'A constant whose value lies between .7 and 1.0

The V_{SL} and V_{SG} terms are the "superficial" velocities of the respective phases, i.e., the velocity each phase would have if that one phase completely filled the tube. Therefore, the superficial velocity of each phase is lower than the average velocity by a factor equal to the respective volume fractions occupied by each phase. If R_L and R_G are the volume fractions for each phase, then

$$V_{SL} = R_L u_L$$

and

$$V_{SG} = R_G u_G$$

Wallis (9) explains the variation in the value of the constant C as being related to the method of introducing liquid into the system, i.e., "end" effects, and also to the degree of disturbance present in the system. In a deep gas well with some of the liquid condensing on the walls, the behavior might be expected to approach that of an infinite system with no end effects. The presence of couplings approximately every 30 feet, however, introduces a large diameter discontinuity in the tube (the "JJ"), creating an effect at every connection. (In patented shouldered thread designs such as Hydril and Atlas Bradford this is not the case, but these are in the minority in the field.) Wallis (9) found the value of C to be .88 in rough finite tubes where large disturbances are present. In the turbulent gas flow field found in gas wells this value should be applicable.

In order to use the flooding equation of Wallis, it is necessary to know the superficial liquid phase velocity. This requires a knowledge of the average film velocity. For the purpose of this analysis where no liquid may accumulate in the bottom of the hole, the film cannot be allowed to achieve a significant velocity anywhere in the conduit. Therefore, the average film velocity is necessarily very small.

Since the superficial liquid velocity is related to the actual velocity by a factor equal to the in situ liquid volume fraction, a quantitative insight into the volume fraction relationships in natural gas wells is necessary. The relative values of the superficial liquid velocities and average film velocities may be determined by applying Hughmark's (14) holdup correlation.

Since in two-phase gas/liquid flow the liquid phase moves with a lower average velocity than the gas, the tubing liquid/gas ratio in situ is higher than the influx or effluent ratios. The increased liquid fraction is called "holdup". Hughmark correlated the holdup with several physical properties and presented a grouping that

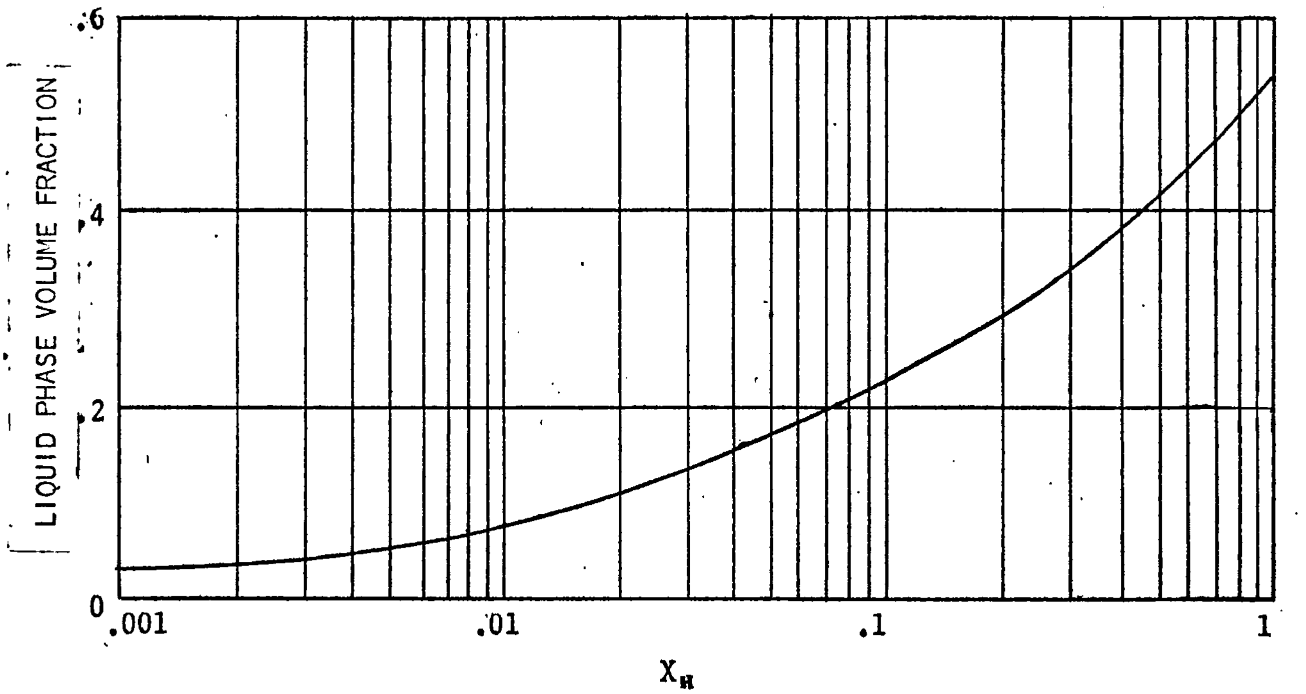

Figure IV

Hughmark's Holdup Correlation

may be used to calculate the liquid volume fraction. The correlating parameter is

$$X_H = 6 \times 10^4 \left[\frac{W_L}{W_G}\right]^{.9} \frac{\mu_L^{.19}\ \sigma^{.205}\ \rho_G^{.70}\ \mu_G^{2.75}}{G^{.435}\ \rho_L^{.72}}$$

where W_L = Liquid mass flow rate

W_G = Gas mass flow rate

σ_L = Interfacial tension

G = Total mass velocity

The term $\left[\frac{W_L}{W_G}\right]$ is the producing liquid/gas ratio in a consistent set of units. Fig. IV shows a plot of X_H vs the liquid phase volume fraction.

For comparison, an average well with liquid production of 25 bbls/MMCF of 50° API condensate at 3000 psia pressure, the value of X will be .009. From Fig. IV, the liquid volume fraction would be 8 per cent. If only 8 per cent of the tubing were filled with the liquid, the superficial film velocity in a flooding model would be 1/12 the average liquid velocity and, therefore, can be assumed to be negligible.

This permits the direct calculation of the gas phase superficial velocity by assuming that V_{SL} equals zero. Eq. 3.06 then reduces to the following simple relationship.

$$V_{SG} = \frac{4.31 \quad D^{\frac{1}{2}} \left(\rho_L - \rho_G \right)^{\frac{1}{2}}}{\rho_G^{\frac{1}{2}}} \qquad 3.09$$

Wallis (25) has studied the effects of liquid viscosity on the flooding equation and found no effect in the correlation if $\overset{*}{V}_G > .5$. Since the assumption is $\overset{*}{V}_G = (.88)^2 = .76$, there should be no viscosity influence.

The calculated superficial gas velocity necessary to flood a falling film may now be used to calculate the gas flow rate. This flow rate represents a minimum flow condition to prevent load up for this possible type of liquid behavior in gas wells.

The Drop Model

In the two previous developments it has been presumed that the liquid is on the walls of the conduit where indeed much of the liquid will be. Some of the liquid, however, will be in the form of droplets in the gas core. The origin of the droplets is of little importance, however some possible mechanisms may be; condensation and subsequent coalescense, wave breakup due to interfacial shear from a larger mass of liquid on the pipe wall or in the coupling "JJ", or as the result of jetting produced formation fluids across the perforation or screen liner slots as the fluid enters the wellbore. This existence of drops in the gas core presents a different problem of liquid transport.

The formation of drops results in particles of roughly spheroidal shape being entrained in the gas stream. The gas flow rate necessary to remove these drops is a function of the properties of both the gaseous and liquid phases, as well as the size and shape of the drops. The linear velocity of the gas at which the largest drops will be suspended motionless is the limiting velocity necessary to remove drops. A velocity incrementally higher will lift the largest, and hence all of the drops out of the wellbore. A velocity slightly lower will lift the smaller drops, but eventually the larger drops will predominate and accumulation will occur. The point at which the largest drops will stagnate or stand still in a moving gas stream is therefore the limiting condition for lifting liquid by a droplet mechanism. The mathematical analysis of this limiting condition may be accomplished using methods from particle dynamics (19).

By transformation of coordinates to a system moving at the same velocity as the gas, the suspension condition is the same as the terminal of "free settling" velocity of the drop in the gravitational field relative to the new coordinate system. This is reached when the drag force caused by the relative motion between the drop and the gas is equal to the accelerating force of gravity.

For a liquid particle falling in a fluid (gas) medium the gravitational force acting on that particle is

$$F_g = \frac{g_L \, Vol \, (\rho_L - \rho_G)}{g_c}$$

where

Vol = Volume of the particle

The drag force resisting the motion of the particle is

$$F_d = \frac{C_d \, A_p \, u_T^2 \rho_G}{2g}$$

where C_d = Drag coefficient

A_p = Projected area of particle

u_T = Velocity of the particle relative to the gas

At the terminal velocity of the particle, these forces are equal, i.e.

$$F_g = F_d$$

$$\frac{g_L \, Vol \, (\rho_L - \rho_o)}{g_c} = \frac{C_d \, A_p \, \rho_G \, u_T^2}{2g}$$

Since the liquid particle takes on a roughly spheroidal shape, this can be rewritten in terms of the drop "diameter" d, and solved for u_T.

$$u_T = 6.55 \sqrt{\frac{d \, (\rho_L - \rho_G)}{C_d \, \rho_G}} \qquad 3.10$$

In order to solve Eq. 3.10 it is necessary to know the drop diameter and the drag coefficient. From Eq. 3.10 it can be seen that the terminal velocity is a direct function of the square root of the drop diameter, therefore, the minimum velocity required to remove all drops will be that which will remove the largest. The problem thus becomes one of determining the maximum drop diameter which can exist in a given shear field. This requires a knowledge of the forces acting on the drops and their interactions.

A liquid drop moving in a gas is subjected to drag forces which tend to deform the drop while surface tension and viscous forces tend to hold it together. Herman (8) presents an analysis of the forces trying to deform and shatter a liquid drop moving relative to a gas phase and concludes that the primary deforming forces is a result of the velocity pressure $\frac{\rho_G u^2}{g_c}$, while the restoring force is provided by the surface tension pressure, $\frac{\sigma_l}{d}$. Hinze (11) states that in drop breakup process, "Two pressures are of importance, the antagonism of which determines the deformation, namely the velocity pressure and the surface tension pressure."

The ratio of these two pressures is the Weber Number

$$N_{We} = \frac{\rho_G u^2 d}{\sigma_l g_c}$$

and is a measure of the relative strength of these two opposing forces. If this ratio exceeds some critical value, the velocity pressure will shatter the drop. Therefore, the largest drop diameter which can exist in a moving gas stream is a function of liquid and gas properties and their relative velocity. The value of this critical Weber Number must be determined experimentally.

Hinze (11, 12) determined the critical Weber Number for drops falling in air and for drops suddenly exposed to high speed air flow. His investigations showed that the critical value of the Weber Number is a function of the accelerating forces acting on the drops. Those drops subjected to a rapid acceleration shattered at lower values of N_{We} than did those falling in the gravitational field. This implies that smaller maximum drop sizes will result for drops formed under conditions of high acceleration such as exists in spray nozzles, etc. For drops falling freely in air, Hinze found the critical Weber Number to be on the order of 15 to 30 although individual determinations varied widely.

In a gas well, liquid drops may be formed by coalescence or condensation and therefore be subjected to slight accelerations. These drops can attain higher Weber Numbers (i.e., larger diameters) than those subjected to sudden accelerations. To prevent load up all drops must be removed, so the largest drops that can exist dictate the minimum gas velocity to accomplish continuous liquid removal. Therefore, using Hinze's upper range value of 30 for the critical Weber Number, the maximum drop diameter becomes

$$d_m = \frac{30 \ \sigma_i \ g_c}{\rho_g \ u^2}$$

This expression for d_m can be substituted into Eq. 3.10.

The only remaining unknown in Eq. 3.10 is the drag coefficient C_d. Hughes and Gilliland (13) developed a correlation for the drag coefficients of liquid drops moving in a gas (Fig. V). In order to use this correlation, values for the drop Reynolds Number

$$N_{Re} = \frac{\rho_G d \; u_T}{\mu_G}$$

and a parameter

$$Su = \frac{g_c \; \sigma_i \; \rho_G \; d}{\mu_G^2}$$

must be obtained.

For application to natural gas wells, the ranges of the above dimensionless groupings can be estimated from known well conditions. Gas velocities known to prevent load up have been shown to be on the order of 5 to 10 ft/sec (3, 24) for high pressure gas wells. Under these conditions gas densities range from 3.4 to 29 lbm/ft^3 and surface tension varies from 60 dynes/cm for water to 15 dynes/cm for condensate. Substituting the expression developed for maximum drop diameter into the definitions for N_{Re} and Su yields

$$N_{Re} = 6.85 \times 10^3 \left[\frac{\sigma_i}{u_T}\right]$$

$$Su = 1.56 \times 10^6 \left[\frac{\sigma_i}{u_T}\right]$$

where σ_i is in dynes/cm and u in ft/sec, the resulting ranges are shown in the following table.

σ_i dynes/cm	u_T ft/sec	$\frac{\sigma}{u_T}$	N_{Re}	Su
60	5	12	8.2×10^4	2.2×10^8
15	10	1.5	1×10^4	3.3×10^6

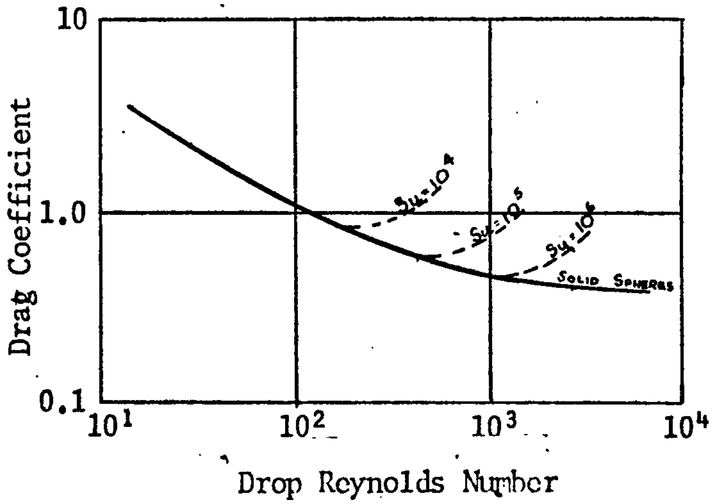

Figure V

Drag Cofficient of Liquid Droplets

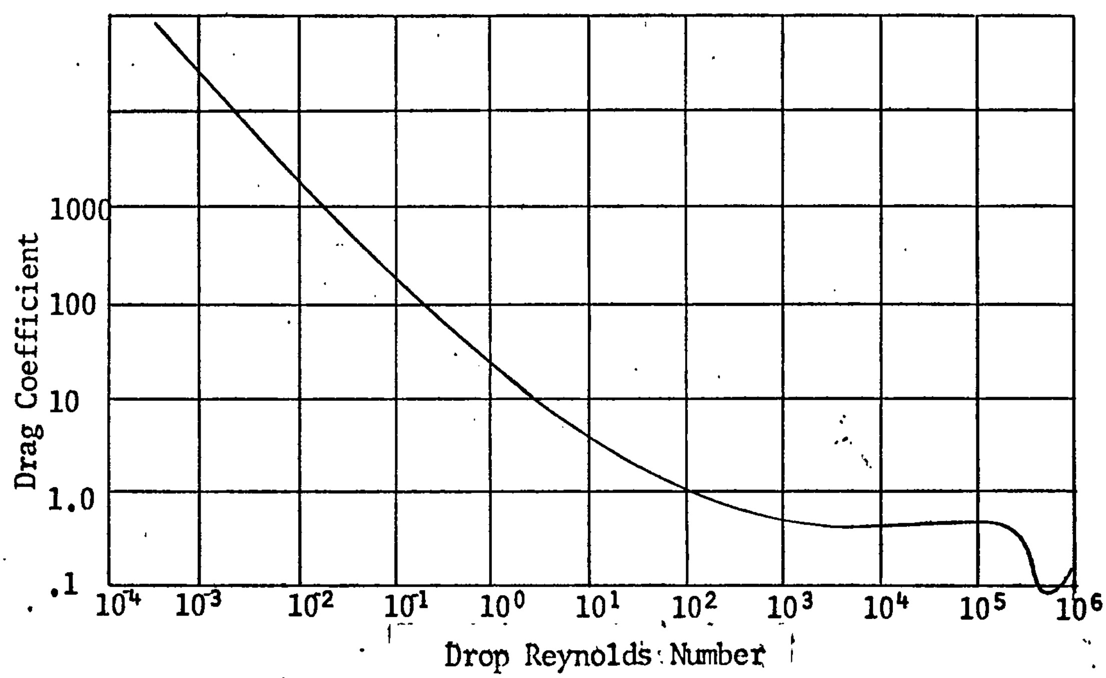

Figure VI

Drag Coefficients of Solid Spheres

These ranges for N_{Re} and Su place the majority of gas wells off of the Hughes and Gilliland correlation of Fig. V. However, the correlation does indicate that, under certain conditions, the drag coefficient for liquid droplets approaches that for solid spheres. Since deformation from the solid sphere shape results in higher drag coefficients and therefore correspondingly lower minimum lift velocities, the solid sphere drag coefficient was chosen as the limiting case. In the Reynolds Number range from 10^3 to 10^5, the solid sphere drag coefficient is approximately constant at a value of 0.44 (Fig. VI) so the value can be assumed as a conservative criterion for predicting minimum lift conditions. Making this substitution, Eq. 3.10 becomes

$$u_T = 17.6 \frac{\sigma_i^{\frac{1}{4}} (\rho_L - \rho_G)^{\frac{1}{4}}}{\rho_G^{\frac{1}{2}}} \qquad 3.11$$

Eq. 3.11 may be used to calculate the minimum gas velocity necessary to remove liquid drops from a gas well.

Chapter IV

LABORATORY INVESTIGATIONS

In order to determine the applicability of the film and/or drop models, an experimental apparatus was constructed in the laboratory which would permit both quantitative as well as qualitative observations to be made concerning the flow.

This laboratory equipment consisted of a 16 foot long pyrex tube, 1.875 inches internal diameter with air and water inlets on a mixing tee. The air was introduced on the run and the water on the side (Fig. VII). Metering and control equipment was used for each phase.

The experimental procedure which was developed involved the establishment of steady state upward co-current flow conditions at some high gas rate sufficient to remove all entering liquids. Steady state was determined when the pressure at the bottom stabilized. The gas rate was reduced in steps allowing equilibrium to be achieved at each rate. As the gas rate decreased, the pressure at the bottom increased due to increased liquid hold up. If the gas rate was sufficient to remove liquids at the same rate at which they were entering, the pressure at the bottom would stabilize. When the gas rate was reduced to a point that it could not remove the liquids, slugging would occur and the pressure would fail to stabilize. This was taken to be the load up point.

The top of the tube was vented to the atmosphere. At the top,

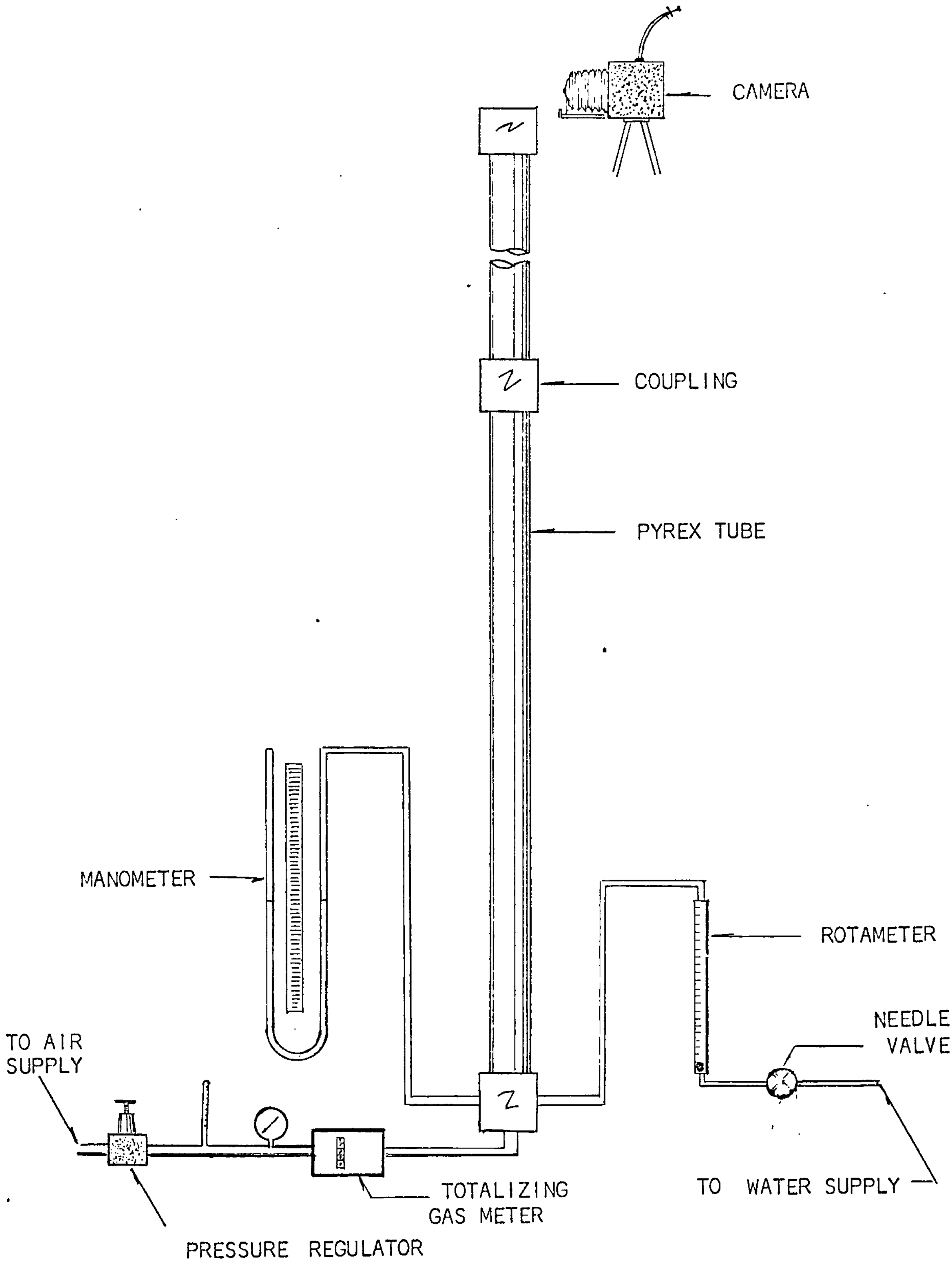

Figure VII

Laboratory Apparatus

observations were made over the complete range of flow rates and high shutter speed still photographs taken of the liquid effluent from the tube (Fig. VIII). In Fig. VIII-A it can be seen that, at the high gas rate, the liquid film is breaking over the top of the tube, shattering into large drops as it does so. As the gas rate is reduced (Fig. VIII-B&C), the film no longer moves over the top of the tube. The entrained droplets continued to be removed from the tube to the point of load up, where the tests were discontinued.

In the intermediate flow rate range between the initial high flows and load up, visual observation of the tube showed significant liquid activity on the walls of the tube. When the rate of gas flow was reduced below that necessary to move the film over the top of the tube, flooding and churning began in the tube. The liquid would try to run down the pipe wall (counter-current), but was almost immediately reversed due to liquid bridging and slug formation. The slugs were quickly penetrated by the gas and liquid drops were torn from the thickened film. Under these conditions the liquid removal was by a drop transport mechanism. Therefore, the film model did not represent the limiting liquid flow condition. As the gas rate was reduced further, the point was reached where the gas was no longer able to remove the liquid as fast as it entered. The liquid build-up in the bottom led to unsteady conditions with the liquid phase being moved in slug form. The pressure at the bottom was erratic and large excursions were noted.

The liquid activity at the coupling was significant in that the

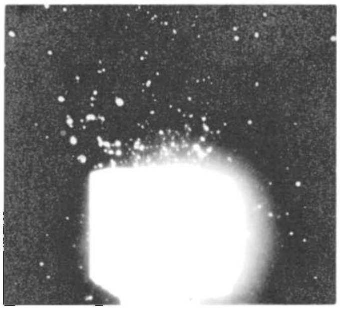

A.
Air Velocity = 60 ft/sec

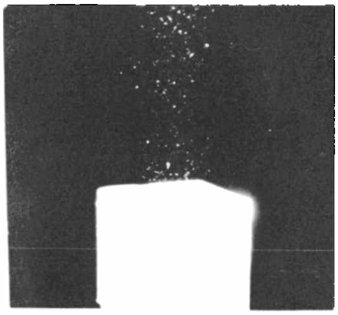

B.
Air Velocity = 40 ft/sec

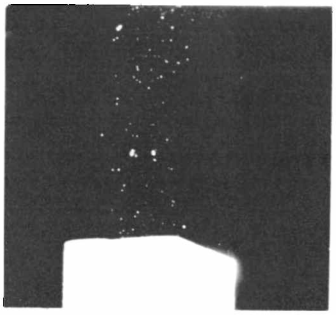

C.
Air Velocity = 30 ft/sec

Figure VIII

The Effect of Gas Velocity
on Drop Removal

discontinuity in the internal diameter caused a localized liquid buildup. The increase in liquid volume fraction in the area of the coupling produced a higher degree of churning than in the rest of the tube, with liquid globules being torn from the larger liquid mass and being redeposited on the walls at a higher elevation.

A two-to-one change in the water/air ratio was used to test the sensitivity of the load up point to gas/liquid ratios. It was observed that for the ratios tested (14 and 33 bbls/mmcf), which is a range normally found in wet gas wells, the minimum gas flow rate showed no dependence on liquid ratio. The data from these runs are given in Table I, and also recorded in the data listings in Appendix D, Table VI.

The laboratory observations gave qualitative insight into the behavior of the liquid phase near the load up point and allowed a preliminary assessment of the flooding and droplet models. The activity on the walls of the tube near the load up point indicated that the liquid will (1) "flood", (2) break into drops to be carried further up the tube, where (3) they will be redeposited on the walls or removed. Therefore, the droplet mechanism is most probably the controlling transport device.

TABLE I

	Gas Flow Rate mmcf/day	Liquid Ratio bbl/mmcf	Test Gas Velocity ft/sec	Calc. Min. Velocity Droplet ft/sec	Calc. Min. Velocity Flooding ft/sec	Flow Condition
Run I	.123	17.5	57.4	39.7	42.5	Unloaded
	.109	14.8	51.3	39.8	42.7	Unloaded
	.084	25.6	40.6	40.4	43.3	Unloaded
	.065	38.2	31.8	40.5	43.6	Loaded
Run II	.122	6.84	56.7	39.6	42.4	Unloaded
	.105	7.95	51.0	40.2	43.0	Unloaded
	.081	10.3	39.2	40.4	43.2	Unloaded
	.058	14.3	28.6	40.9	43.6	Loaded

Chapter V

COMPARISONS WITH FIELD DATA

Sources and Types of Data

The data used for testing the correlations were obtained from actual wells in gas fields across the country. Some data were the result of tests performed specifically to determine the minimum flow rate that would continuously remove liquids. Other data came from wells that were known to be incapable of removing the liquid and in fact were equipped with artificial lift devices to maintain constant gas production. Still other data came from wells that had been flowing steadily and removing a constant liquid rate. These data bracket the minimum lift condition sufficiently to enable its determination.

Included in the data are the two most commong flow geometrics, standard production tubing in API sizes and annular completions where the gas is flowed between the casing and the tubing (single string dual completions).

The conduit sizes included in the data range from 1.750 inches I.D. (2-1/16" O.D. tubing) to 8 inch diameter casing. Several annular areas are included with both 5-1/2" and 7" O.D. casings being represented.

Liquid phase material included salt water and condensate ranging in API gravity from 43° to 70°.

Some of the data are incomplete for the purpose of this investigation, and it is necessary to estimate the values of some properties. These include:

Interfacial Tension This property is not usually determined in routine analysis and it was therefore not obtainable for the individual well fluids. The surface tension of water was obtained from a handbook (16), and the surface tension of the hydrocarbon liquids was taken from a correlation with molecular weight (18).

Bottom Hole Temperature Some of the data were incomplete and the bottom hole temperatures were not reported. In these cases estimates were made from area geothermal gradient charts, since the location and depth of the wells were known.

Density of the Liquid Phase and Gravity of the Gas These quantities are very important to the developments and, unfortunately, were not available for some of the data. The data that were insufficient in this respect did, however, contain the liquid/gas ratio. It is generally true that in wells that produce a small quantity of liquid, the liquid will be a clear, very light (high API gravity) volatile liquid, with a correspondingly light (low gravity) gas. Conversely, a rich or high liquid/gas ratio well will generally have more dense liquid and gas phases. From these principles and a knowledge of the ranges of these quantities normally encountered in the field, approximations were made. In the case of water, the specific gravity was taken to be 1.08, the specific gravity of 28,000 ppm salt water, a value found in many areas. (This is the concentration of sea water and many fields contain marine environment water.)

In Situ Gas/Liquid Ratio The pressure and temperature at the bottom of the hole (Fig. IX, Point B) may be above the "dew point", that condition of the hydrocarbon mixture which is analagous to saturation in soluble two-component systems. This means that only single phase material is entering the wellbore. As this material moves up the conduit, the pressure and temperature are reduced and the mixture becomes saturated (Point D). From this point as the pressure and temperature are reduced further, more liquid is formed.

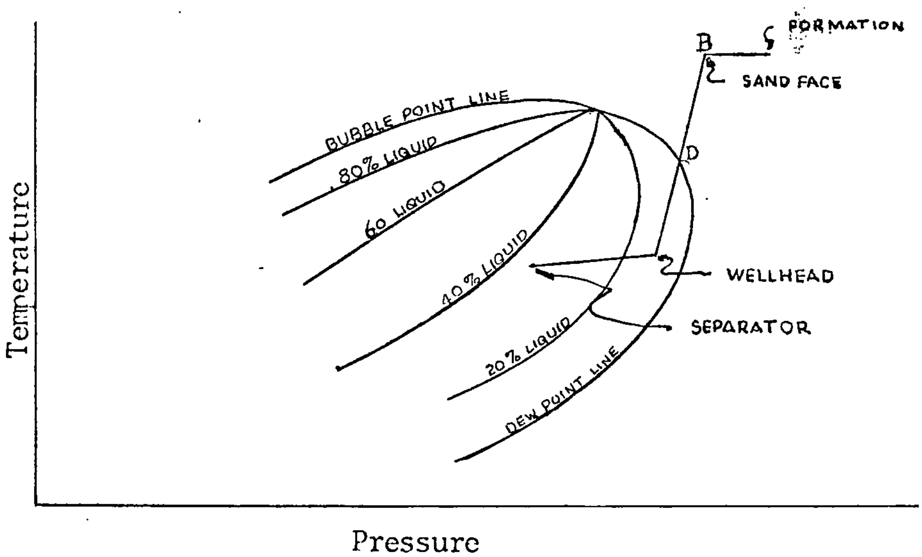

Figure IX

Phase Diagram of Typical Gas Condensate System

The remainder of the produced liquid is formed in the surface separation facility. Since in normal field observations only the total liquid production is reported, the quantity which was actually present or formed in the tubing is indeterminate. In general, the largest quantity is probably present near the wellhead. In this study, the total liquid production was assumed to form in the wellbore or before entry into it.

Many of the data were obtained through producing companies from the well test data. A portion was taken from the paper by Duggan (4), and other points were published by Rawlins and Schellhardt (19).

The three developments derived in Chapter III may be tested individually against field data, but each of the three models require a value for the gas phase density in the calculation procedure. This quantity, which is a function of the pressure, temperature and the gravity of the gas, varies over the entire length of the conduit. It is necessary to determine the point in the conduit where the maximum flow rate is required to remove liquids. For comparative purposes the correlations are tested at the two extremes, i.e., at the wellhead and at the bottom of the hole.

Since the data were for the most part obtained for purposes other than determining the minimum flow rates necessary to prevent load up, a circumstance develops that deserves careful attention. The comparison of the calculated flow rates with the observed flow rates in this instance does not lead to a grouping of points on a line that represents the validity of a correlation. The technique used here is directed toward separating what are known to be adequate flow rates from those which are known to be inadequate such that the grouping of parameters will prove the flow rate of a well to be sufficient to lift liquids. The interdependency of flow rate and pressure in gas wells requires a trial and error procedure to predict the minimum flow rate. The individual deliverability (ability to produce) of each well must be considered to predict the minimum condition.

The grouping of points in Figs. X through XIII are not expected to fall on a line, but rather to show a separation between those wells which were known to load up and those which were known to have flowed without liquid accumulation. The line on the plot represents the loci of points where the test flow rate is equal to the calculated flow rate. If a point falls above the line, it means that the flow rate in the field was above the minimum flow rate calculated by the respective correlations. The converse is true for points below the line.

Comparison with Individual Models

Film Model The development of the film model imposed several restrictions on its application. These are: (1) a tubular conduit (as opposed to an annular configuration), and (2) a system containing gas and a single liquid phase either condensate or water, but not both. The applicable data were processed and the results listed in Table II and plotted in Fig. X. The higher of the predicted flow rates from the two extremes of the conduit were used.

The results indicate that the film model predicts flow rates that are considerably higher than those observed to be satisfactory for continuous liquid removal in the field. For wells with similar pressures and conduit size but different gas/liquid ratios, significantly different calculated minimum flow rates are predicted. This gas/liquid ratio sensitivity is inconsistent with field observations which show no such dependency. The film model is therefore presumed to not be the controlling mechanism for liquid recovery from gas

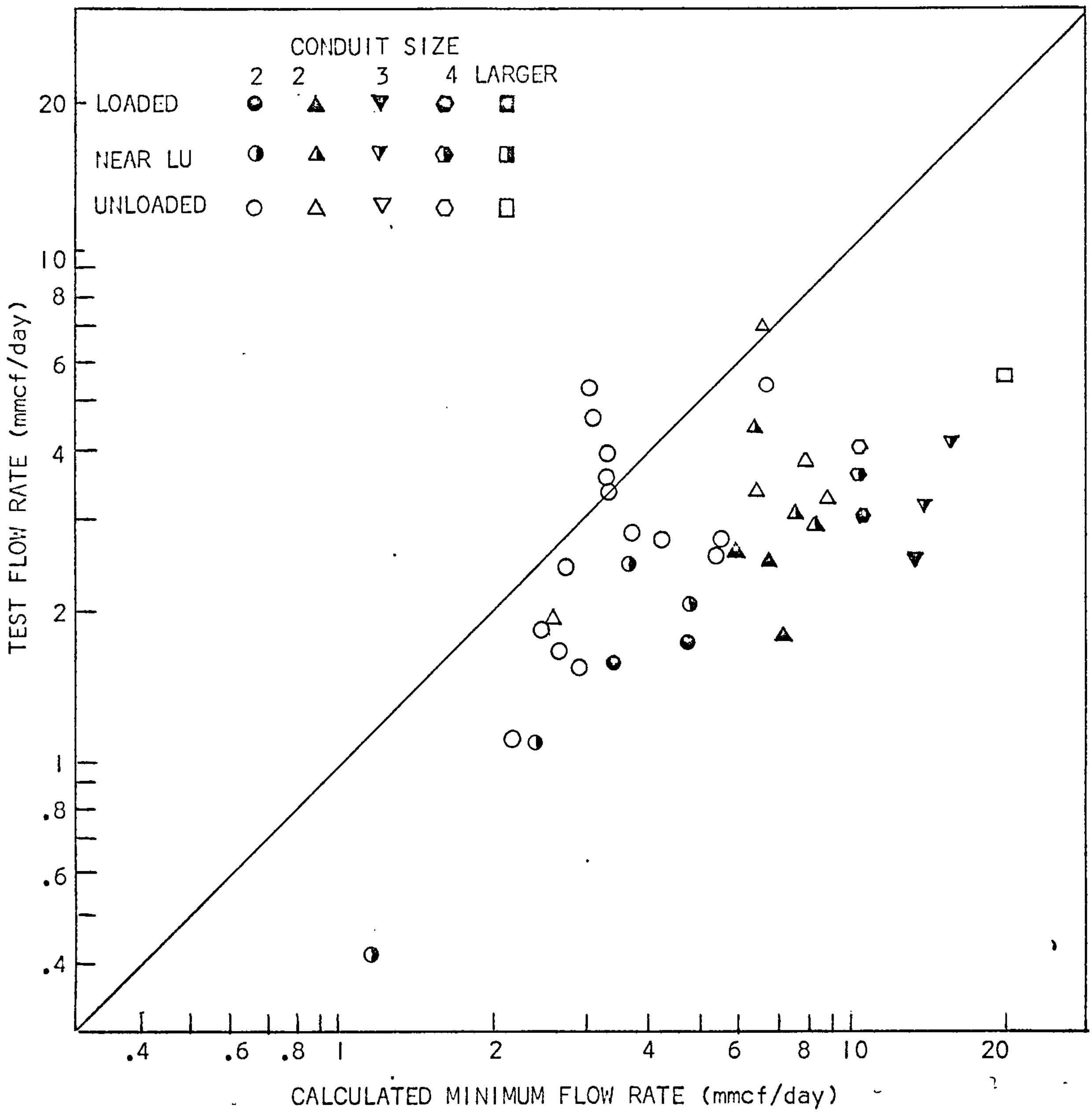

Figure X

Comparison of Field Tests with Film Model wells. This is in agreement with the laboratory tests discussed previously.

Flooding Model The flooding model, which is an empirical correlation, is also restricted to tubular geometries and a single liquid phase. The correlation has not been extended to other flow areas and immiscible multi-phase liquids. Only those data meeting these conditions were processed and the results are presented in Table III. These data were plotted (Fig. XI) in the same form as the film model. The calculated minimum flow rates in the smaller conduit sizes show relatively good separation of the data. In the large conduits, however, unreasonably high minimum flow rates were predicted, indicating that the model was not generally applicable.

Drop Model The drop model is not restricted to a tubular conduit nor does the development require a single liquid phase, therefore, all data could be tested. In those wells producing both water and condensate, the higher density and surface tension of the water were considered to be controlling properties. The minimum flow rates were calculated using Eq. 3.11 and the results are presented graphically in Fig. XII and listed in Table IV. The separation of the data is generally good. However, for some of the data, the predicted minimum flow rate is still below that which is believed to be inadequate from field tests. This is perhaps due to the definition of load up applied by the various data sources.

The individual sources utilized different techniques for deciding whether or not a well was loading up. Some of the data were

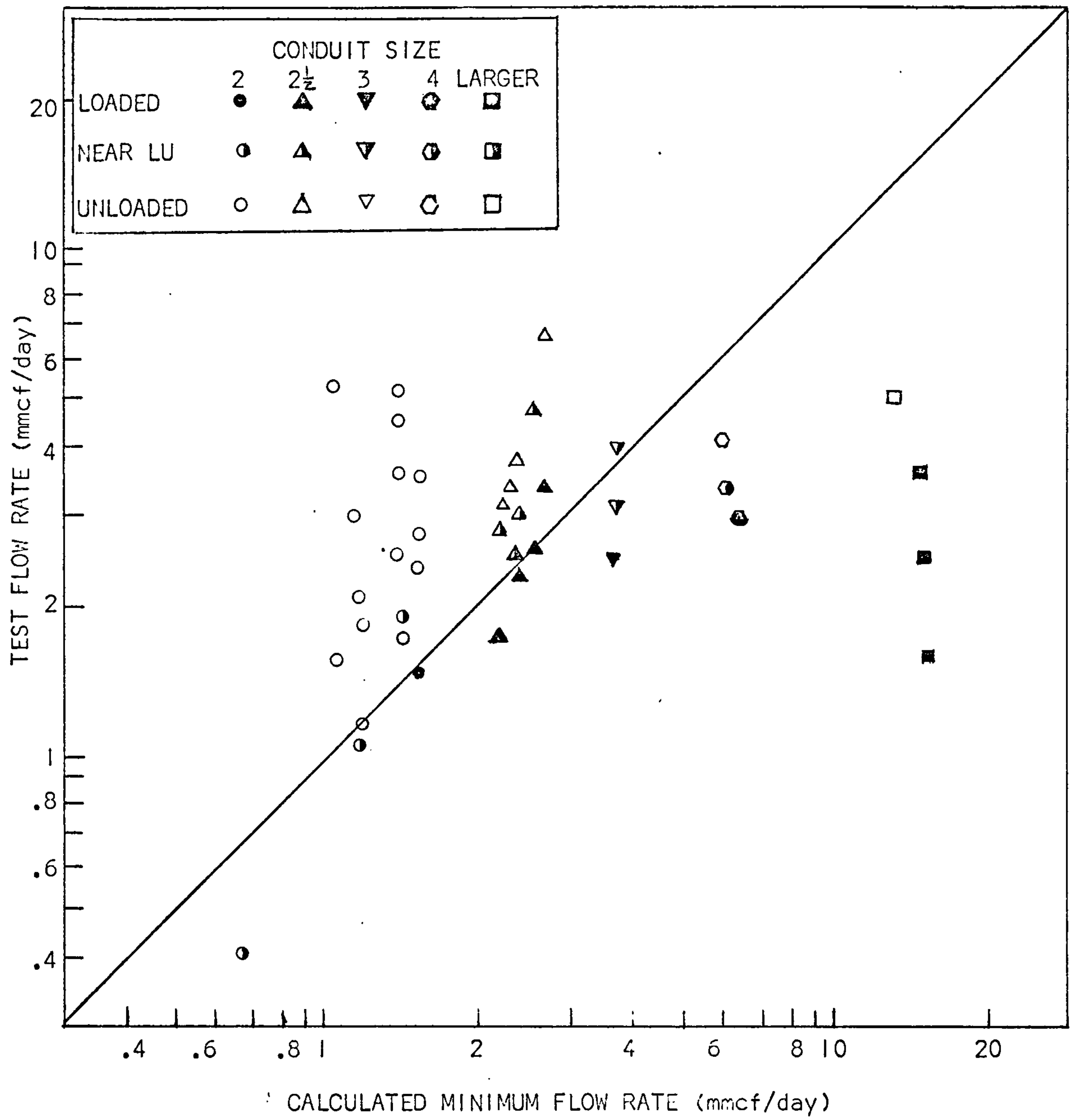

Figure XI

Comparison of Field Tests with Flooding Model evaluated by the calculated $(P_F^2 - P_S^2)$ term in the back pressure test, the position of a test point on the back pressure test curve being indicative of the condition of liquid accumulation. Other data were from wells that accumulated liquids to the point of cessation of gas flow.

In order to achieve a development which will satisfactorily predict the minimum flow rate consistent with all of the field definitions of load up, an adjustment may be made in the correlation. The value of the critical Weber Number was taken from widely varying experimental data determined in a laboratory under conditions other than exists in a gas well. In a long conduit containing discontinuities in the internal diameter (couplings) and high density gas flowing at relatively low velocities, the liquid drops are exposed to conditions which are significantly different from those falling in quiescent air. The value of the critical Weber Number may be different for drops under these circumstances. By changing the value of this empirically determined quantity, it is possible to utilize the drop model to predict minimum gas flow rates for liquid removal that better agree with all of the field observations without changing the theoretical development. A value of $N_{We}(crit) = 60$ was found to give the best agreement with all of the data. The results of the calculation using this value are shown in Fig. XIII and Table V.

The drop model therefore allows calculation of the minimum gas flow rate necessary to continuously remove liquids from gas wells by application of individual well parameters. This method lends itself

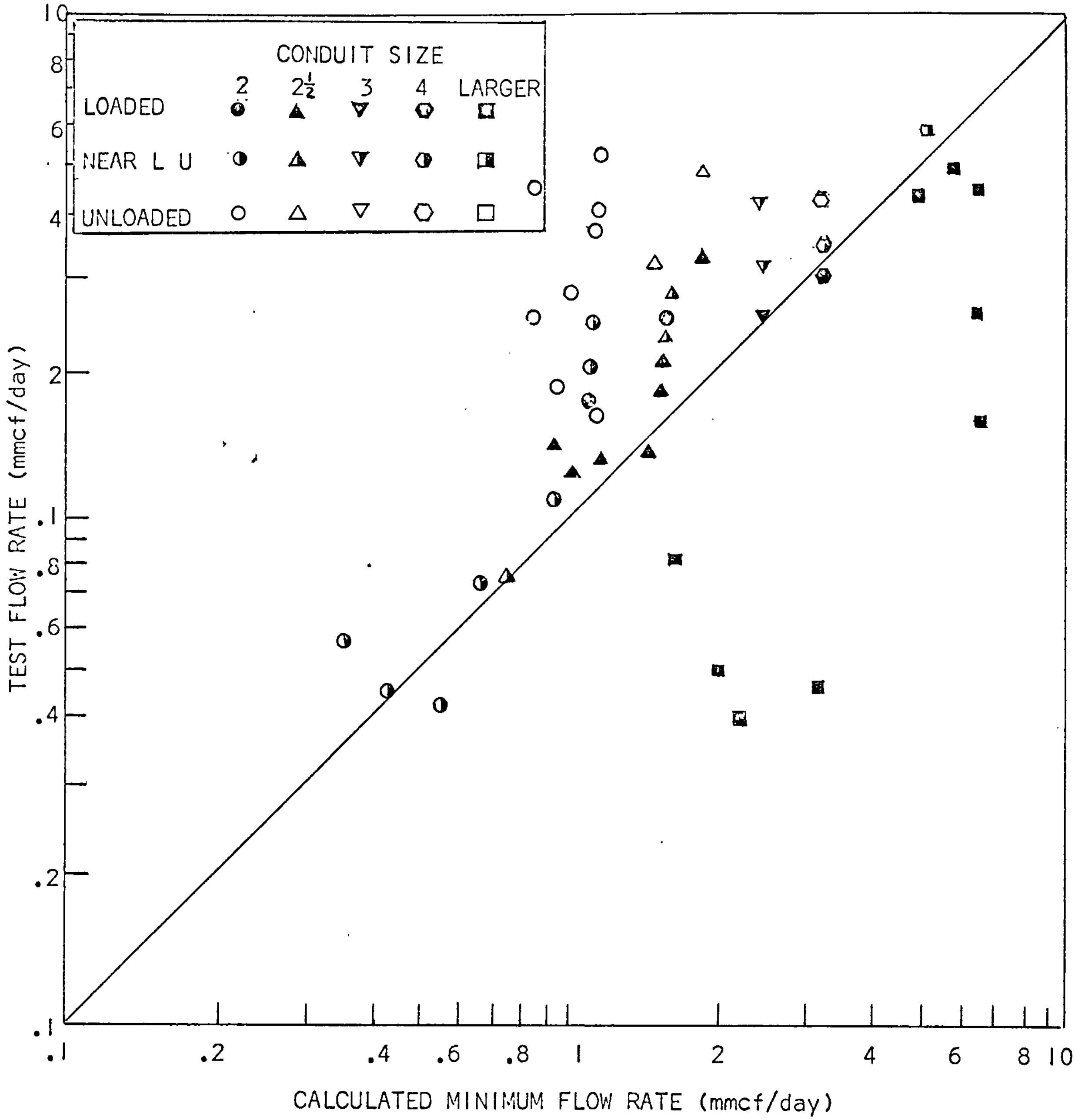

Figure XII

Comparison of Field Tests with Drop Model ($N_{We(crit)} = 30$)

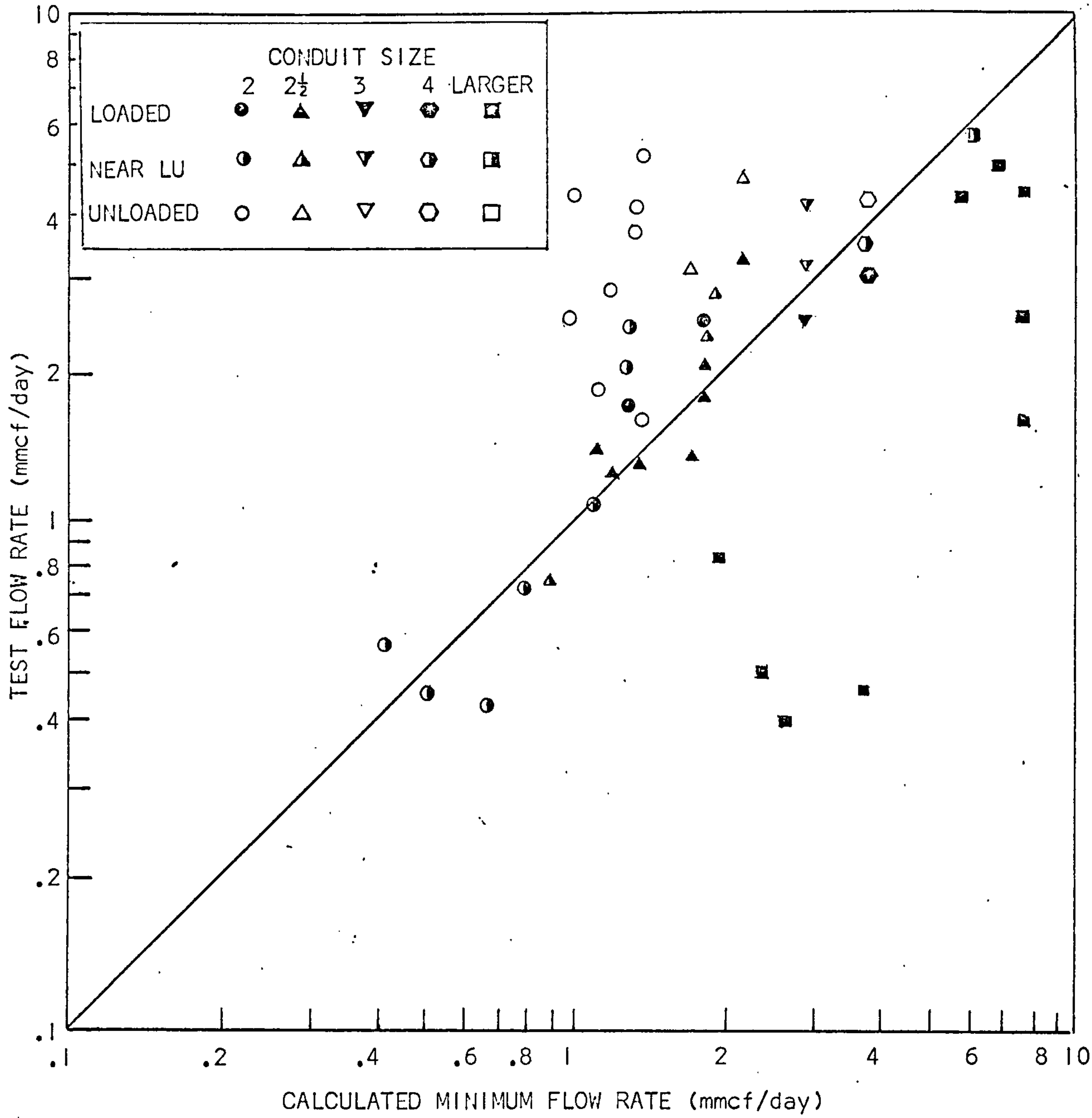

Figure XIII

Comparison of Field Tests with Drop Model ($N_{We(CRIT)}$=60) to graphical solution as is presented in Appendix A.

The comparison of the three models indicates that the controlling mechanism for liquid removal in gas wells is that of moving the largest liquid drops that can exist up the conduit. The calculations indicate that only in a few instances are there significant differences in the minimum rate calculated at the surface from that calculated at the bottom of the hole. The larger of the flow rates was not found to be consistently at either end. For general application the surface conditions are satisfactory for use in the equations and in the graphical solution.

Chapter VI

CONCLUSIONS

The correlations developed for film movement, flooding film behavior and drop movement in a vertical gas stream when tested against laboratory and field observations indicate that the limiting gas flow rate necessary to continuously remove liquids from a gas well is that rate which will remove the largest liquid drops that can exist in the moving gas stream. The film model predicts flow rates significantly higher than field observation and also reveals gas liquid ratio sensitivity not found in the field data. The flooding model shows relatively good agreement with field observation in small diameter conduits, however, in large diameter conduits, the predicted flow rates are much too high. The drop model provides a satisfactory calculation procedure for determining the minimum gas flow rate for continuous liquid removal in any flow configuration.

The results of this study indicate that the following equations are adequate to predict the minimum flow rate necessary to continuously remove liquids from gas wells.

Minimum gas velocity

$$u = \frac{20.9 \quad [\sigma_L(\rho_L - \rho_G)]^{\frac{1}{4}}}{\rho_G^{\frac{1}{2}}} \qquad 6.01$$

Minimum gas flow rate

$$Q_{min} = \frac{3.06 \ P \ u \ A}{T \ Z} \qquad 6.02$$

For field application, a nomograph has been prepared for solution of these equations which appears in Appendix A.

BIBLIOGRAPHY

1. Calvert, Seymour and Williams, Brymer. Uwards Co-Current Annular Flow of Air and Water in Smooth Tubes. A.I.Ch.E. Journal, Vol. I, No. I, March, 1965. P. 78.

2. Craft, B. C. and Hawkins, M. F. Applied Petroleum Reservoir Engineering. Prentice Hall. 1959. P. 325.

3. Duggan, J. O. Estimating Flow Rate Required to Keep Gas Wells Unloaded. Journal of Petroleum Technology, December, 1961. P. 1173.

4. Dukler, A. E. Fluid Mechanics and Heat Transfer in Vertical Falling Film Systems. Chemical Engineering Progress, Vol. 56, No. 30, 1960.

5. ____________ Design of Multi-Phase Flow Systems. Presented at API Southwestern District Meeting, Albuquerque, N. M. March, 1961.

6. Flaitz, J. M. and Parks, A. S. Sampling Gas Condensate Wells. Petroleum Technology (TP 1374), Vol. 4, No. 4, 1941.

7. Gill, W. N. and Scher, M. A Modification of the Momentum Transport Hypothesis. A.I.Ch.E. Journal, Vol. 7, No. 1, March, 1961. P. 61.

8. Herman, J. Flow Properties of Disperse Systems. North Holland Publishing Co., Amsterdam. 1963. P. 310.

9. Hewitt, G. F. Analysis of Annular Two-Phase Flow: Application of the Dukler Analysis to a Vertical Upward Flow in a Tube. A.E.R.E. R-3680. 1961.

10. ____________ and Wallis, G. B. Flooding and Associated Phenomenon in Falling Film Flow in a Tube. A.E.R.E. R-4033. 1963.

11. Hinze, J. O. Fundamentals of the Hydrodynamic Mechanism of Splitting in Dispersion Processes. A.I.Ch.E. Journal, Vol. I, No. 3, September, 1955. P. 289.

12. ____________ Critical Speeds and Sizes of Liquid Globules. Applied Scientific Research, Vol. A-1. P. 273.

13. Hughes, R. R. and Gilliland, E. R. The Mechanics of Drops. Chemical Engineering Progress, No. 48. 1952. P. 497.

14. Hughmark, C. A. and Pressberg, B. S. Holdup and Pressure Drop with Gas Liquid Flow in a Vertical Pipe. A.I.Ch.E. National Meeting. 1959.

15. Jones, Park J. Petroleum Production, Vol. 3 . 1947. P. 100.

16. Lange's Handbook of Chemistry, Eighth Edition. 1942. P. 1615.

17. Lockhart, R. W. and Martinelli, R. C. Proposed Correlation of Data for Isothermal Two-Phase, Two-Component Flow in Pipes. Chemical Engineering Progress, Vol. 45, No. 1, January, 1949. P. 39-48.

18. Natural Gasoline Supply Men's Association Engineering Data Book. 1951. P. 144

19. Perry, J. H. Chemical Engineers Handbook, Fourth Edition, McGraw-Hill. 1963. P. 5-50.

20. Rawlins, E. L. and Schellhardt, M. A. Back Pressure Data on Natural Gas Wells and Their Application to Production Practices. U. S. Bureau of Mines Monograph No. 7. 1935. P. 34.

21. Roxburgh, Chas. D. M. S. Thesis. University of Houston. 1962.

22. Smith, R. V. Open Flow of Gas Wells. Petroleum Production Handbook. McGraw-Hill. 1962. P. 30-8.

23. Stanton, Ralph G. Numerical Methods for Science and Engineering. Prentiss Hall. 1965.

24. Vitter, A. L. Back Pressure Tests on Gas-Condensate Wells. A.P.I. Drilling and Production Practice. 1942. P. 79.

25. Wallis, G. B. The Influence of Viscosity on Flooding in a Vertical Tube. Report No. 62GL132, General Electric Laboratory, August, 1962.

APPENDIX

APPENDIX A

Application to Field Design

For field application it is highly desirable to have a simple method to determine the minimum flow rate necessary to insure continuous liquid removal. Although the equations required to calculate this quantity are not particularly complex, a slide rule or logarithm tables are necessary. It is, therefore, worthwhile investigating methods of simplifying the equations.

Since, from the conclusions reached in Chapter IV and V, we presume that drop removal is the limiting liquid removal mechanism, the Eq. 6.01 for terminal drop velocity will be used for the field application. The grouping of parameters are such that we can simplify the equation to a relationship suitable for graphical solution.

Since the fourth root of the surface tension of low molecular weight hydrocarbons varies only slightly with changes in molecular weight and temperature, a consolidation of the $\sigma^{\frac{1}{4}}$ term into a constant for condensates is indicated. For water, another constant may be used. The liquid phase density for condensates will vary between 51.5 lbm (40° API) and 43.8 (70° API). Therefore, the liquid phase density for condensates (which is also involved in a fourth root extraction) may be treated as a constant. Water will also have a roughly constant density.

This leaves two equations (one each for water and condensate) in which the terminal velocity is a function of the pressure, temperature and gas gravity. A plot of the calculated minimum gas velocities for the wells tested versus pressure, (Fig. XIV) shows very little deviation from the straight line. The deviation is, of course, due to temperature and gravity variations, but due to the limited overall spread (on an absolute scale) of these quantities, little variation is experienced. This plot then allows the construction of a nomograph by which a test point may be quickly checked for adequate liquid removal. The interdependency of flow rate and pressure precludes having a direct flow rate calculation. Instead, unless a performance curve (back pressure test) is already available, it is necessary to observe the flow rate and the pressure, utilize the nomograph and determine if that flow rate is adequate. The utilization of wellhead pressures are generally sufficient for this purpose. If the bottom hole flowing pressure is known, the rate at that point might be checked for adequacy.

Calculation Procedure

For field application, the following adjusted equations may be used.

For wells producing water,

$$u_G = \frac{5.62 \ (67 - .0031P)^{\frac{1}{4}}}{(.0031P)^{\frac{1}{2}}}$$

For wells producing condensate only,

$$u_G = \frac{4.02 \ (45 - .0031P)^{\frac{1}{4}}}{(.0031P)^{\frac{1}{2}}}$$

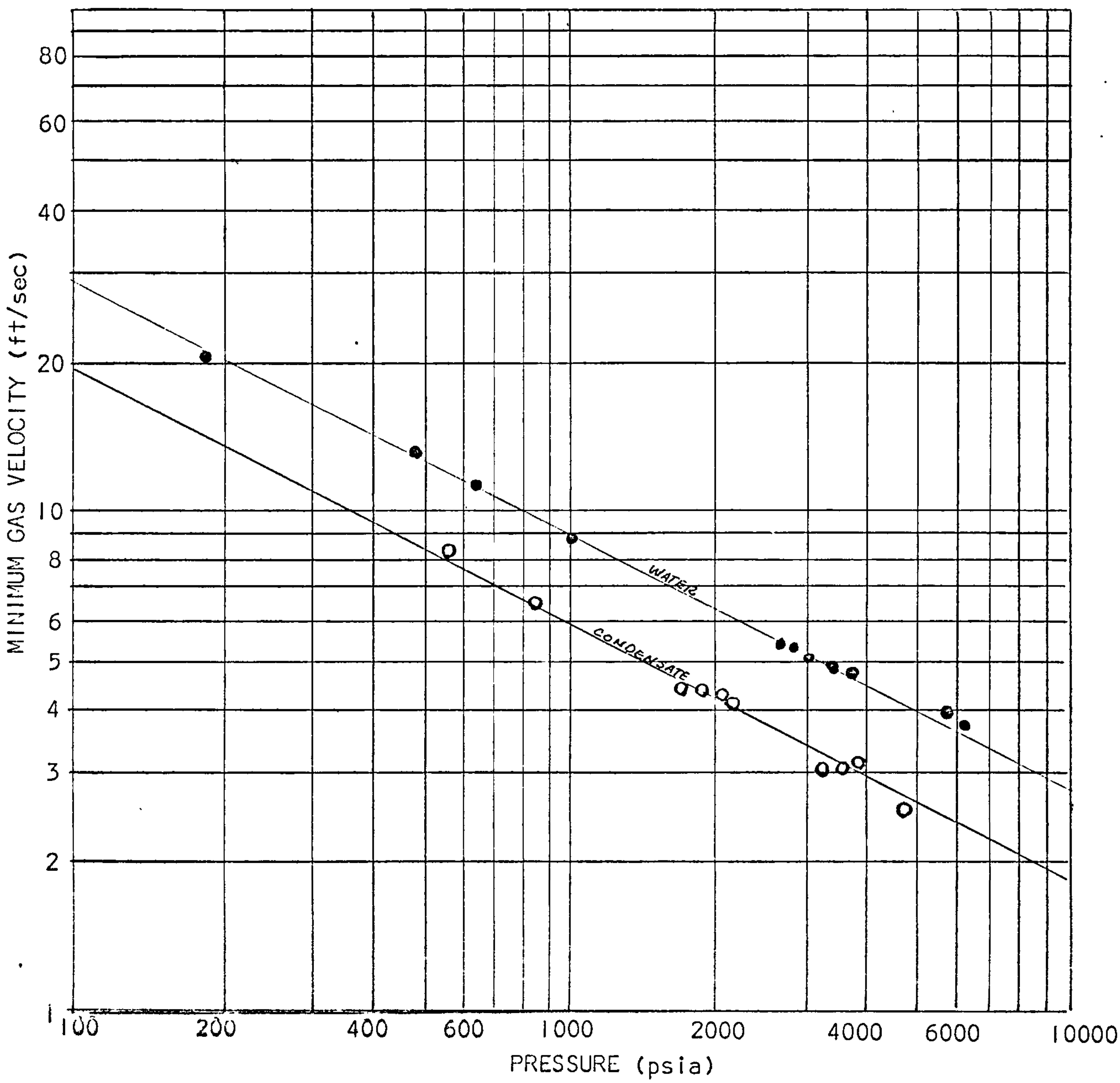

Figure XIV

Minimum Gas Velocity vs Pressure

The minimum flow rate may then be calculated by

$$Q_{mm} = \frac{3.06\ P\ u\ A}{T\ Z}$$

The nomograph allows consideration of all values in the above equation except the deviation Z. Resulting information from the nomograph is the product QZ. For more accurate flow rates, the Z factor must be divided into the QZ term.

The nomograph is used by starting at the pressure of interest, going vertical to the properline, and then horizontal to the edge of the grid. This is the minimum gas velocity. From this point a line is drawn through the $\frac{P}{T}$ line to the intermediate line, and from this line through the flow area line to the QZ line.

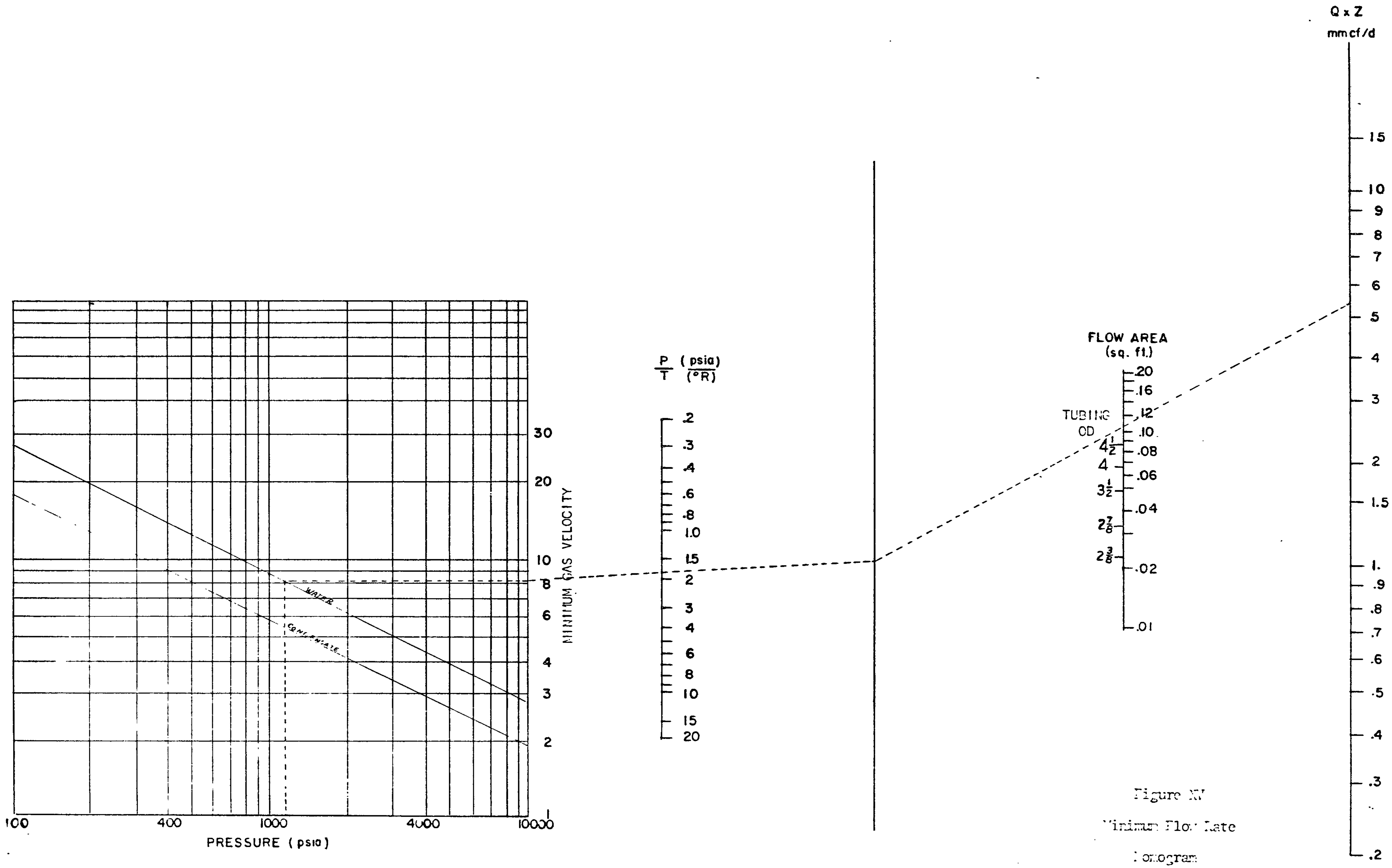

Figure XV

Minimum Flow Rate

Nomogram

Appendix B

JONES' MINIMUM FLOW RATE EQUATION

The limiting gas velocity necessary to move a liquid drop upward in a flowing gas stream is the maximum velocity the drop would attain if allowed to free fall in a static system of equivalent properties. This terminal velocity is found by the following equations.

$$u = \sqrt{\frac{2\, g_L d\, (\rho_L - \rho_G)}{3\, C_d\, \rho_G}} \qquad 1$$

where u = The terminal velocity of the drop

d = The drop diameter

C_d = The drag coefficient

ρ_L = The drop density

ρ_G = The gas density

g = The local gravitational acceleration

Jones reasoned that in a pipe of diameter D, the largest drop that could exist was one with that same diameter D. He also assumed that the density difference, $(\rho_L - \rho_G)$, was relatively constant at approximately 62 lbm/ft^3. Therefore, Eq. 1 reduces to

$$u = 37.4\sqrt{\frac{D}{\rho_G\, C_d}}$$

since

$$\rho_G = \frac{P\, M}{R\, T\, Z}$$

$$u = 122\sqrt{\frac{D\, T\, Z}{M\, P\, C_d}}$$

The flow rate of gas expressed in terms of velocity, pressure and temperature is

$$Q = \frac{3.06\ P\ u\ A}{T\ Z}$$

For a round tube

$$A = \frac{\pi\ D^2}{4}$$

$$Q = \frac{2.40\ P\ D\ 122}{T\ Z}\sqrt{\frac{DTZ}{PMC_d}}$$

$$= \frac{298}{C_d}\ D^{\frac{5}{2}}\left(\frac{P}{M\ T\ Z}\right)^{\frac{1}{2}}$$

Changing D to inches and equating C to .44

$$Q = 1.0\ D^{\frac{5}{2}}\left(\frac{P}{M\ T\ Z}\right)^{\frac{1}{2}}$$

Jones' published equation shows a 1.5 constant which Jones [illegible] stated did not belong in the equation. The published version also shows the deviation factor, Z, to be squared. It is the author's opinion that this is a misprint.

Appendix C

THE FILM MODEL

For steady state conditions to exist in a system of gas/liquid vertical co-current flow with the liquid contained in an annular film surrounding the gas core, the upward forces must equal the downward forces, i.e., an overall force balance must exist. For a differential element of thickness dx, at any point y distance from the wall, the upward acting force is the shear stress, τ, acting on the area π (D-2y) dx.

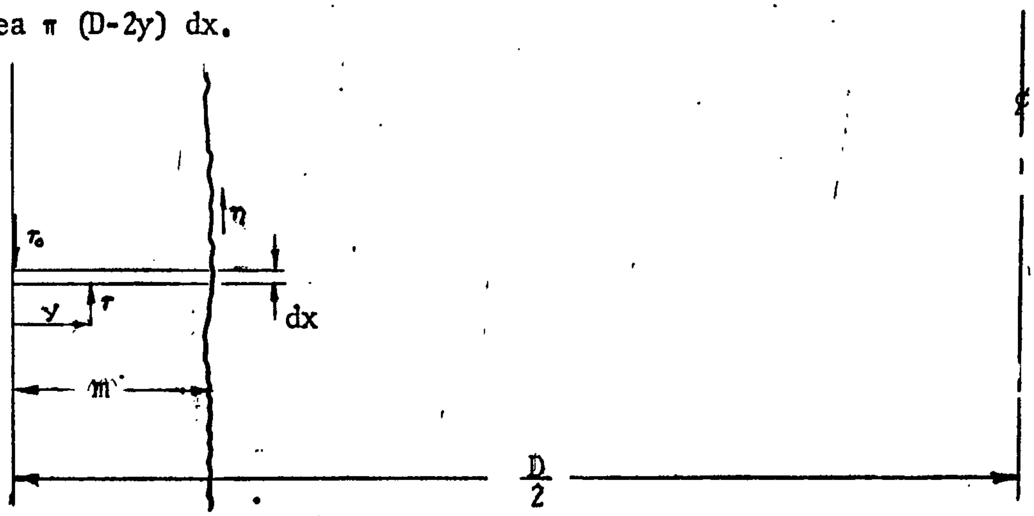

$$F\uparrow = \tau\pi (D - 2y) dx \qquad 1$$

In thin films the value of y in the film is small compared to the diameter of the tube, and so the quantity 2y is insignificant compared to D. Therefore

$$F\uparrow = \tau \pi D dx \qquad 2$$

The shear stress at the wall, τ_o, is resisting the movement of the film, as is the gravitational attraction on the mass of liquid. The shear stress at the wall is acting on the area πDdx, and the mass of liquid resisting the force provided by τ is approximately $\pi Dydx\rho_L$. The forces acting in the downward direction are therefore

$$F_o\downarrow = \tau_o \ \pi \ D \ dx \tag{3}$$

and

$$F_G\downarrow = \pi \ D y \rho_L \frac{g_L}{g_c} dx \tag{4}$$

Since, for steady state, the forces must be equal

$$F\uparrow = F_o\downarrow + F_G\downarrow \tag{5}$$

$$\tau \pi D \, dx = \tau_o \pi D dx + \pi D y \ \rho_L \frac{g_L}{g_c} dx \tag{6}$$

$$\frac{\tau}{\tau_o} = 1 + \frac{y \rho_L g_L}{\tau_o \ g_c} \tag{7}$$

The introduction of several parameters is necessary at this point

$$u^* = \sqrt{\frac{\tau_o \ g_c}{\rho_L}} \tag{8}$$

$$u^+ = \frac{u}{u^*} \tag{9}$$

where u is the velocity at any point in the film

$$y^+ = \frac{y u^* \rho_L}{\mu_L} \tag{10}$$

u^* is the "friction velocity" and u^+ and y^+ are dimensionless velocity and distance parameters respectively.

Since

$$y = \frac{\mu_L \ y^+}{u^* \rho_L} \tag{11}$$

and

$$\tau_o = \frac{u^{*2}\rho_L}{g_c} \qquad 12$$

Eq. 7 becomes

$$\frac{\tau}{\tau_o} = 1 + \frac{y\,\mu_L\,g}{u^{*3}\rho_L} \qquad 13$$

The distance parameter evaluated at the gas liquid interface is

$$\eta = \frac{m u^{*}\rho_L}{\mu_L} \qquad 14$$

Defining another parameter

$$\sigma = \frac{m}{b} \qquad 15$$

where

$$b^3 = \frac{\eta^2\mu_L^2}{\rho_L^2 g_L} \qquad 16$$

Therefore Eq. 15 becomes

$$\sigma^3 = \frac{m^3\rho_L^2 g_L}{\eta^2\mu_L^2} \qquad 17$$

and

$$\frac{\sigma^3}{\eta} = \frac{m^3\rho_L^2 g_L}{\eta^3\mu_L^2} \qquad 18$$

or

$$\frac{\sigma^3}{\eta} = \frac{\mu_L g_L}{u^{*3}\rho_L} \qquad 19$$

Therefore Eq. 13 becomes

$$\frac{\tau}{\tau_o} = 1 + y^+ \frac{\sigma^3}{\eta} \qquad 20$$

From fluid mechanics, the total shear stress equation for laminar and turbulent flow is

$$g_c \tau = (\mu_L + \xi \rho_L) \frac{du}{dy} \qquad 21$$

where $\xi \rho_L$ is the eddy viscosity term, and du/dy is the velocity gradient. This equation can be transformed into dimensionless form by using Eq. 9 and 10

$$u^+ = \frac{u}{\sqrt{\frac{\tau_o g_c}{\rho_L}}} \qquad 22$$

$$u = u^+ \sqrt{\frac{\tau_o g_c}{\rho_L}} \qquad 23$$

$$du = du^+ \sqrt{\frac{\tau_o g_c}{\rho_L}} \qquad 24$$

Similarly

$$y = \frac{y^+ \mu_L}{\rho_L \sqrt{\frac{\tau_o g_c}{\rho_L}}} \qquad 25$$

$$dy = dy^+ \frac{\mu_L}{\rho_L \sqrt{\frac{\tau_o g_c}{\rho_L}}} \qquad 26$$

$$\frac{du}{dy} = \frac{du^+}{dy^+} \frac{\rho_L \left(\sqrt{\frac{\tau_o g_c}{\rho_L}}\right)^2}{\mu_L} \qquad 27$$

$$\frac{du}{dy} = \frac{du^+}{dy^+} \frac{\tau_o g_c}{\mu_L} \qquad 28$$

Eq. 21 now becomes

$$\tau = \left(\mu_L + \xi\rho_L\right)\frac{\tau_o}{\mu_L}\;\frac{du^+}{dy^+} \tag{29}$$

$$\frac{\tau}{\tau_o} = \left(1 + \frac{\xi}{\nu}\right)\frac{du^+}{dy^+} \tag{30}$$

where ν is the kinematic viscosity.

The evaluation of $\frac{\xi}{\nu}$ in terms of the other parameters is accomplished by the use of the Gill and Scher equation (6). This equation is valid for all vales of y, from the wall to the center of the tube

$$\frac{\xi}{\nu} = k^2 y^{+2}\left(1 - e^{-\phi\frac{y^+}{y_m^+}}\right)^2 \frac{du^+}{dy^+} \tag{31}$$

$$y_m^+ = \frac{u^* D \rho_L}{2\mu_L} \tag{32}$$

$$\phi = \frac{y_m^+ - 60}{22} \tag{33}$$

$$k = .36 \tag{34}$$

The total shear stress equation is therefore

$$\frac{\tau}{\tau_o} = \left[1 + k^2 y^{+2}\left(1 - e^{-\phi\frac{y^+}{y_m^+}}\right)^2\frac{du^+}{dy^+}\right]\frac{du^+}{dy^+} \tag{35}$$

Equating 30 and 35

$$1 + y^+\frac{\sigma^3}{\eta} = \left[1 + k^2 y^{+2}\left(1 - e^{-\phi\frac{y^+}{y_m^+}}\right)^2\frac{du^+}{dy^+}\right]\frac{du^+}{dy^+} \tag{36}$$

By substitution let

$$D = \frac{du^+}{dy^+} \qquad 37$$

$$A = k^2 y^{+2} \left(1 - e^{-\phi \, y^+ / y_m^+} \right)^2 \qquad 38$$

$$C = 1 + y^+ \frac{\sigma}{\eta} \qquad 39$$

Eq. 36 becomes

$$C = (1 + AD) D \qquad 40$$

$$AD^2 + D - C = 0 \qquad 41$$

$$D = \frac{-1 \pm \sqrt{1 + 4AC}}{2A} \qquad 42$$

Since $D = \frac{du}{dy}$ and the gradient is always positive, disregard the negative root

$$D = \frac{-1 + \sqrt{1 + 4AC}}{2A} \qquad 43$$

Multiplying by $\frac{-1 - \sqrt{1 + 4AC}}{-1 - \sqrt{1 + 4AC}}$ 44

$$D = \frac{-1 - (1 + 4AC)}{-2A \left(1 + \sqrt{1 + 4AC} \right)} \qquad 45$$

$$D = \frac{2C}{1 + \sqrt{1 + 4AC}} \qquad 46$$

Therefore

$$u^+ = \int_0^{y^+} \frac{2\left(1 + y^+ \frac{\sigma^3}{\eta}\right)}{1 + \sqrt{1 + 4\left(k^2 y^{+2}\left(1 - e^{-\phi \frac{y^+}{\sqrt{\eta}}}\right)^2\left(1 + y^+ \frac{\sigma^3}{\eta}\right)\right)}} dy^+ \qquad 47$$

Eq. 47 is the dimensionless velocity distribution in the film. The liquid mass flow rate of the film can be obtained by the integral

$$W_L = \pi D \mu_L \int_0^{\eta} u^+ dy^+ \qquad 48$$

Re-examining a differential element across the tube

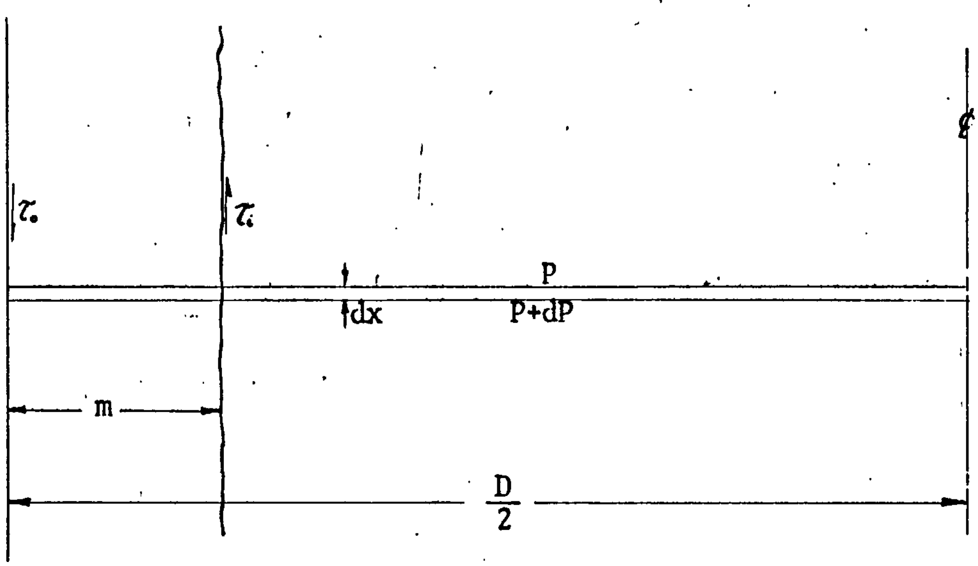

It is necessary at this point to perform an overall steady state force balance on the entire cross-section. The total force in the downward direction is

$$F = \tau_o \pi D\, dx + \pi D\, m\, \rho_L \frac{g_L}{g_c} dx + \frac{\pi D^2}{4} \rho_G \frac{g_L}{g_c} dx \qquad 49$$

The total force in the upward direction is a result of the pressure drop, d P

$$F = \frac{\pi D^2}{4} dP \tag{50}$$

$$F = \frac{\pi D^2}{4} \frac{dP}{dx} dx \tag{51}$$

Equating 49 and 51

$$\tau_o = \left(\frac{dP}{dx} - \rho_G \frac{g_L}{g_c}\right)\frac{D}{4} - m \rho_L \frac{g_L}{g_c} \tag{52}$$

Defining

$$\frac{dP}{dx}_{TP} = \frac{dP}{dx} - \rho_L \frac{g_L}{g_c} \tag{53}$$

Eq. 53 equals the frictional pressure gradient or two-phase pressure drop.

Eq. 52 becomes

$$\tau_o = \frac{dP}{dx}_{TP} \frac{D}{4} - m \rho_L \frac{g_L}{g_c} \tag{54}$$

Introducing the parameter

$$F = \frac{\frac{dP}{dx}_{TP}}{\rho_L \frac{g_L}{g_c}} \tag{55}$$

$$\tau_o = \rho_L \frac{g_L}{g_c} \left(F \frac{D}{4} - m \right) \tag{56}$$

$$\tau_o = \frac{\eta^2 \mu_L^2}{m^2 \rho_L g_L} \tag{57}$$

$$\tau_o \quad \frac{b^3 \rho_L g_L}{m^2 g_c} \tag{58}$$

or

$$\frac{b^3}{m^2} = F\frac{D}{4} - m \qquad 59$$

Dividing both sides of Eq. 59 by $\frac{b^3}{m^2}$ and substituting from Eq. 16 and Eq. 17

$$1 = \frac{F\,D\,\sigma^2 \rho_L^{\frac{2}{3}} g_L^{\frac{1}{3}}}{4\,\mu_L^{\frac{2}{3}}\,\eta^{\frac{2}{3}}} \qquad 60$$

Defining

$$\beta = \frac{F\,D\,\rho_L^{\frac{2}{3}} g_L^{\frac{1}{3}}}{4\,\mu_L^{\frac{2}{3}}} \qquad 61$$

and substituting in 60

$$\sigma^3 - \left(\frac{\beta}{\eta^{\frac{2}{3}}}\right)\sigma^2 + 1 = 0 \qquad 62$$

The interfacial shear stress

$$\tau_i = \frac{dP}{dx_{tp}}\frac{D}{4} \qquad 63$$

$$\tau_o = \tau_i - m\,\rho_L \frac{g_L}{g_c} \qquad 64$$

$$\tau_o = \frac{\eta^2 \mu_L^2}{m\,\rho_L\,g_L} \qquad 65$$

By substitution in Eq.17

$$\sigma^3 = \frac{\frac{m\,\rho_L \frac{g_L}{g_c}}{\tau_i}}{1 - \frac{m\,\rho_L \frac{g_L}{g_c}}{\tau_i}} \qquad 66$$

Let

$$X = \frac{m\,\rho_L \frac{g_L}{g_c}}{\tau_i} \qquad 67$$

The X is actually the ratio of the "gravitational shear force", $m \rho_L \frac{g_L}{g_c}$, to the interfacial shear force, τ_i. In vertical co-current upward flow, the minimum gas phase velocity for continuous film movement in the upward direction is that which will provide a value of τ_i that is incrementally greater than $m \rho_L \frac{g_L}{g_c}$, i.e., the value of X must be slightly less than one. For purposes of this analysis, we take the value of X = .99

$$\sigma^3 = \frac{X}{1 - X} \qquad 68$$

$$\sigma = \left(\frac{.99}{1 - .99}\right)^{\frac{1}{3}} \qquad 69$$

Since $$\sigma = \frac{X^{\frac{1}{3}}}{(1 - X)^{\frac{1}{3}}} \qquad 70$$

By substitution in Eq. 62

$$\frac{X}{1 - X} - \frac{\beta}{\eta^{\frac{1}{3}}} \frac{X^{\frac{2}{3}}}{(1 - X)^{\frac{2}{3}}} + 1 = 0 \qquad 71$$

or

$$\frac{\beta}{\eta^{\frac{1}{3}}} = \frac{1}{X^{\frac{2}{3}}(1 - X)^{\frac{1}{3}}} \qquad 72$$

For X = .99

$$\frac{\beta}{\eta^{\frac{1}{3}}} = 4.67 \qquad 73$$

The method of applying the above equations involves an iterative solution and requires the use of a digital computer. It is necessary to assume a flow rate and proceed to calculate through the development to a calculated flow rate. The calculated flow rate must be made to converge to the assumed flow rate.

For evaluation of all the quantities it is necessary to know the two-phase pressure drop, $\frac{dP}{dx}_{TP}$. This is accomplished by use of the Lockhart and Martinelli correlation (16).

$$\Phi_G = 3.3\, X^{.22} \tag{74}$$

$$\Phi_G = \sqrt{\frac{\frac{dP}{dx}_{TP}}{\frac{dP}{dx}_{G}}} \tag{75}$$

$$X = \sqrt{\frac{\frac{dP}{dx}_{L}}{\frac{dP}{dx}_{G}}} \tag{76}$$

$$\frac{\frac{dP}{dx}_{TP}}{\frac{dP}{dx}_{G}} = 10.89 \left(\frac{\frac{dp}{dx}_{L}}{\frac{dP}{dx}_{G}}\right)^{.22} \tag{77}$$

$$\frac{dP}{dx}_{TP} = 10.89\, \frac{dP}{dx}_{G} \left(\frac{\frac{dP}{dx}_{L}}{\frac{dP}{dx}_{G}}\right)^{.22} \tag{78}$$

$$\frac{dp}{dx}_{L} = \frac{32\, W_L\, f_L}{\pi^2 D^5 g_L \rho_L} \tag{79}$$

$$\frac{dp}{dx}_{G} = \frac{32\, W_G\, f_G}{\pi^2 D^5 g_L \rho_G} \tag{80}$$

The values of f_G and f_L (the Fanning Friction Factors) may be found by

$$f_G = .0014 + \frac{.125}{N_{ReG}^{.32}} \qquad 81$$

$$f_L = .0014 + \frac{.125}{N_{ReL}^{.32}} \qquad 82$$

The N_{Re} parameters are the Reynolds Moduli

$$N_{ReG} = \frac{4W_G}{\pi D \mu_G} \qquad 83$$

and

$$N_{ReL} = \frac{4W_L}{\pi D \mu_L} \qquad 84$$

The solution to the equations requires the use of a digital computer since the integrals are to complex to integrate using classical methods. The equations were programmed in Fortran IV for the IBM 7094 Computer.

TABLE II

THE FILM MODEL

WELL NO	CALCULATED FLOW RATE SURFACE	CALCULATED FLOW FLOW BOTTOM	TEST FLOW RATE	FLOW CONDITION
21	1098	1043	417	NEAR L.U.
61	3453	3008	1525	LOADED UP
62	3866	3397	2926	UNLOADED
71	3811	3368	2494	NEAR L.U.
72	4235	3791	3726	UNLOADED
81	13028	11900	2611	LOADED UP
82	14199	12993	3264	NEAR L.U.
83	15511	14223	4095	NEAR L.U.
91	7247	6532	1814	LOADED UP
92	8551	7779	2915	NEAR L.U.
93	8347	7635	2915	UNLOADED
101	4780	4307	1792	LOADED UP
102	5410	4996	2572	UNLOADED
111	7952	7217	2261	LOADED UP
112	8212	7452	2503	NEAR L.U.
113	8992	8263	3351	UNLOADED
121	4916	4541	2069	NEAR L.U.
122	5505	5100	2769	UNLOADED
131	6867	6496	2542	LOADED UP
132	7439	7063	3182	NEAR L.U.
133	8040	7652	3890	UNLOADED
141	6057	5728	2547	LOADED UP
142	6580	6256	3517	UNLOADED
151	6495	6108	3472	LOADED UP
152	6524	6150	4896	NEAR L.U.
153	6676	6282	6946	UNLOADED
161	2563	2390	1116	NEAR L.U.
162	2504	2366	1959	UNLOADED
181	10983	10307	3009	LOADED UP
182	10820	10183	3551	NEAR L.U.
183	10711	10110	4150	UNLOADED
271	2276	2185	1138	UNLOADED
281	2652	2521	1797	UNLOADED
282	2863	2770	2502	UNLOADED
283	3108	3087	3460	UNLOADED
284	3309	3371	4439	UNLOADED
285	6953	7402	5656	UNLOADED
301	2155	2038	2939	UNLOADED
302	2097	2023	4140	UNLOADED
303	1953	2011	5820	UNLOADED
304	1884	2010	6871	UNLOADED
361	3336	1343	3322	UNLOADED
362	3265	1331	3809	UNLOADED
363	3175	1317	4634	UNLOADED
364	3024	1298	5422	UNLOADED
381	2900	1124	1540	UNLOADED
382	2913	1125	2439	UNLOADED

THE FILM MODEL

WELL NO	CALCULATED FLOW RATE SURFACE	CALCULATED FLOW FLOW BOTTOM	TEST FLOW RATE	FLOW CONDITION
383	2954	1131	3436	UNLOADED
384	2881	1152	4471	UNLOADED
391	2801	1053	1550	UNLOADED
392	2697	1027	1804	UNLOADED
393	2512	985	2385	UNLOADED
394	2246	926	2949	UNLOADED
421	19974	10514	5740	NEAR L.U.

TABLE III

THE FLOØDING MØDEL

WELL NØ	CALCULATED MINIMUM FLØW RATES		TEST FLØW RATE	FLØW CONDITIØN
	SURF MCFD	BØTTØM MCFD	MCFD	
11	1151	1145	775	NEAR L.U.
21	659	630	417	NEAR L.U.
31	351	404	568	NEAR L.U.
41	746	728	712	NEAR L.U.
51	558	538	442	NEAR L.U.
61	1436	1325	1525	LØADED UP
62	1418	1312	2926	UNLØADED
71	1441	1343	2494	NEAR L.U.
72	1427	1337	3726	UNLØADED
81	3685	3501	2611	LØADED UP
82	3672	3490	3264	NEAR L.U.
83	3666	3488	4095	NEAR L.U.
91	2244	2121	1814	LØADED UP
92	2210	2093	2915	NEAR L.U.
93	2181	2069	2915	UNLØADED
101	1376	1301	1792	LØADED UP
102	1356	1297	2572	UNLØADED
111	2245	2124	2261	LØADED UP
112	2232	2110	2503	NEAR L.U.
113	2195	2085	3351	UNLØADED
121	1361	1303	2069	NEAR L.U.
122	1354	1297	2769	UNLØADED
131	2308	2239	2542	LØADED UP
132	2302	2237	3182	NEAR L.U.
133	2296	2234	3890	UNLØADED
141	2258	2183	2547	LØADED UP
142	2220	2151	3517	UNLØADED
151	2572	2524	3472	LØADED UP
152	2564	2515	4896	NEAR L.U.
153	2557	2503	6946	UNLØADED
161	1234	1173	1116	NEAR L.U.
162	1204	1155	1959	UNLØADED
181	5958	5664	3009	LØADED UP
182	5878	5600	3551	NEAR L.U.
183	5815	5551	4150	UNLØADED
251	1402	1491	8672	UNLØADED
252	1578	1562	6654	UNLØADED
253	1640	1596	5136	UNLØADED
254	1675	1618	3917	UNLØADED

THE FLOODING MODEL

WELL NO	CALCULATED MINIMUM FLOW RATES		TEST FLOW RATE	FLOW CONDITION
	SURF MCFD	BOTTOM MCFD	MCFD	
261	1918	1777	3376	UNLOADED
262	1884	1770	4830	UNLOADED
263	1859	1764	6221	UNLOADED
264	1817	1756	7792	UNLOADED
271	1086	1054	1138	UNLOADED
272	1044	1018	1712	UNLOADED
273	970	957	2473	UNLOADED
274	894	897	2965	UNLOADED
281	1116	1075	1797	UNLOADED
282	1098	1071	2502	UNLOADED
283	1067	1061	3460	UNLOADED
284	1034	1049	4439	UNLOADED
285	990	1039	5656	UNLOADED
291	1271	1181	1596	UNLOADED
292	1233	1150	2423	UNLOADED
293	1130	1082	3598	UNLOADED
294	977	1002	4410	UNLOADED
301	1017	978	2939	UNLOADED
302	999	974	4140	UNLOADED
303	949	969	5820	UNLOADED
304	921	967	6871	UNLOADED
311	1216	1151	1943	UNLOADED
312	1134	1099	2910	UNLOADED
313	1033	1040	3742	UNLOADED
314	939	997	4485	UNLOADED
331	1515	1440	2688	UNLOADED
332	1488	1433	3585	UNLOADED
333	1454	1424	4380	UNLOADED
334	1469	1463	5270	UNLOADED
341	1756	1614	2700	UNLOADED
342	1685	1556	3176	UNLOADED
343	1633	1525	3925	UNLOADED
344	1569	1486	4619	UNLOADED
361	1512	1455	3322	UNLOADED
362	1493	1443	3809	UNLOADED
363	1468	1423	4634	UNLOADED
364	1421	1394	5422	UNLOADED
371	1704	1608	2873	UNLOADED
372	1679	1603	4200	UNLOADED

THE FLOODING MODEL

WELL NO	CALCULATED MINIMUM FLOW RATES SURF MCFD	BOTTOM MCFD	TEST FLOW RATE MCFD	FLOW CONDITION
373	1639	1603	6077	UNLOADED
374	1591	1605	7992	UNLOADED
381	1382	1309	1540	UNLOADED
382	1390	1305	2439	UNLOADED
383	1404	1297	3436	UNLOADED
384	1377	1291	4471	UNLOADED
391	1322	1239	1550	UNLOADED
392	1289	1215	1804	UNLOADED
393	1226	1167	2385	UNLOADED
394	1127	1087	2949	UNLOADED
411	1459	1369	1247	LOADED UP
412	1398	1317	1313	LOADED UP
413	1519	1421	1356	LOADED UP
414	1792	1649	1365	LOADED UP
415	1221	1178	1607	LOADED UP
421	13450	13304	5740	NEAR L.U.
422	15613	15411	3890	LOADED UP
423	16299	16079	2780	LOADED UP
424	16747	16515	1638	LOADED UP

TABLE IV

THE DROP MODEL

CRITICAL WEBER NUMBER = 30

WELL NO	CALCULATED MINIMUM FLOW RATES		TEST FLOW RATE	FLOW CONDITION
	SURF MCFD	BOTTOM MCFD	MCFD	
11	779	776	775	NEAR L.U.
21	583	557	417	NEAR L.U.
31	306	352	568	NEAR L.U.
41	661	645	712	NEAR L.U.
51	419	404	442	NEAR L.U.
61	1156	1042	1525	LOADED UP
62	1150	1042	2926	UNLOADED
71	1158	1056	2494	NEAR L.U.
72	1142	1050	3726	UNLOADED
81	2412	2254	2611	LOADED UP
82	2401	2245	3264	NEAR L.U.
83	2395	2243	4095	NEAR L.U.
91	1635	1515	1814	LOADED UP
92	1600	1490	2915	NEAR L.U.
93	1572	1468	2915	UNLOADED
101	1108	1026	1792	LOADED UP
102	1085	1022	2572	UNLOADED
111	1623	1509	2261	LOADED UP
112	1610	1496	2503	NEAR L.U.
113	1574	1475	3351	UNLOADED
121	1091	1029	2069	NEAR L.U.
122	1082	1022	2769	UNLOADED
131	1660	1593	2542	LOADED UP
132	1654	1591	3182	NEAR L.U.
133	1648	1589	3890	UNLOADED
141	1604	1536	2547	LOADED UP
142	1569	1508	3517	UNLOADED
151	1956	1883	3472	LOADED UP
152	1941	1871	4896	NEAR L.U.
153	1930	1856	6946	UNLOADED
161	936	883	1116	NEAR L.U.
162	910	868	1959	UNLOADED
171	3767	4046	5501	LOADED UP
172	3757	4123	6405	NEAR L.U.
173	3747	4222	7504	UNLOADED
181	3281	3106	3009	LOADED UP
182	3233	3068	3551	NEAR L.U.
183	3195	3040	4150	UNLOADED
191	4920	4879	4441	LOADED UP

7 4

THE DROP MODEL

CRITICAL WEBER NUMBER = 30

WELL NO	CALCULATED MINIMUM FLOW RATES SURF MCFD	BOTTOM MCFD	TEST FLOW RATE MCFD	FLOW CONDITION
192	4793	4767	4843	LOADED UP
193	4649	4646	5513	UNLOADED
201	5931	5986	8185	LOADED UP
202	5902	5969	9039	NEAR L.U.
203	5857	5945	9897	UNLOADED
211	6082	6064	6702	LOADED UP
212	6015	6016	8210	NEAR L.U.
213	5957	5974	9289	UNLOADED
221	5580	5577	7109	LOADED UP
222	5559	5588	8406	NEAR L.U.
223	5535	5602	9747	UNLOADED
231	5641	5659	6361	LOADED UP
232	5671	5721	8057	NEAR L.U.
233	5485	5600	9860	UNLOADED
234	5212	5434	11767	UNLOADED
241	3613	3803	4124	LOADED UP
242	3412	3763	4998	NEAR L.U.
243	3199	3836	6423	UNLOADED
251	1239	1324	8672	UNLOADED
252	1407	1392	6654	UNLOADED
253	1467	1424	5136	UNLOADED
254	1502	1446	3917	UNLOADED
261	1770	1616	3376	UNLOADED
262	1732	1609	4830	UNLOADED
263	1705	1602	6221	UNLOADED
264	1659	1593	7792	UNLOADED
271	851	823	1138	UNLOADED
272	814	791	1712	UNLOADED
273	750	739	2473	UNLOADED
274	686	689	2965	UNLOADED
281	875	839	1797	UNLOADED
282	859	836	2502	UNLOADED
283	832	827	3460	UNLOADED
284	803	816	4439	UNLOADED
285	765	807	5656	UNLOADED
291	1216	1122	1596	UNLOADED
292	1176	1090	2423	UNLOADED
293	1070	1021	3598	UNLOADED
294	918	942	4410	UNLOADED

75

THE DROP MODEL

CRITICAL WEBER NUMBER = 30

WELL NO	CALCULATED MINIMUM FLOW RATES SURF MCFD	BOTTOM MCFD	TEST FLOW RATE MCFD	FLOW CONDITION
301	834	797	2939	UNLOADED
302	817	794	4140	UNLOADED
303	770	789	5820	UNLOADED
304	746	787	6871	UNLOADED
311	899	847	1943	UNLOADED
312	833	806	2910	UNLOADED
313	755	760	3742	UNLOADED
314	683	727	4485	UNLOADED
331	1352	1280	2688	UNLOADED
332	1327	1273	3585	UNLOADED
333	1294	1265	4380	UNLOADED
334	1299	1294	5270	UNLOADED
341	1578	1438	2700	UNLOADED
342	1507	1382	3176	UNLOADED
343	1457	1353	3925	UNLOADED
344	1394	1316	4619	UNLOADED
351	9490	8839	4242	UNLOADED
352	9423	8799	5050	UNLOADED
353	9300	8743	6111	UNLOADED
354	9156	8656	7571	UNLOADED
361	1184	1129	3322	UNLOADED
362	1166	1117	3809	UNLOADED
363	1141	1099	4634	UNLOADED
364	1097	1072	5422	UNLOADED
371	1523	1430	2873	UNLOADED
372	1499	1425	4288	UNLOADED
373	1460	1425	6077	UNLOADED
374	1414	1427	7992	UNLOADED
381	1062	998	1540	UNLOADED
382	1069	995	2439	UNLOADED
383	1082	988	3436	UNLOADED
384	1058	983	4471	UNLOADED
391	1026	952	1550	UNLOADED
392	996	931	1804	UNLOADED
393	941	890	2385	UNLOADED
394	856	824	2949	UNLOADED
401	5098	4761	3024	UNLOADED
402	5045	4740	3863	UNLOADED
411	1148	1076	1247	LOADED UP

7

THE DRØP MØDEL

CRITICAL WEBER NUMBER = 30

WELL NO	CALCULATED MINIMUM FLOW RATES		TEST FLØW RATE	FLØW CØNDITIØN
	SURF MCFD	BØTTØM MCFD	MCFD	
412	1099	1034	1313	LØADED UP
413	1197	1118	1356	LØADED UP
414	1419	1303	1365	LØADED UP
415	958	924	1607	LØADED UP
421	5093	5038	5740	NEAR L.U.
422	5923	5845	3890	LØADED UP
423	6186	6102	2780	LØADED UP
424	6359	6270	1638	LØADED UP
441	2184	2214	400	LØADED UP
451	1726	1788	800	LØADED UP
461	6367	6354	4300	LØADED UP
471	2083	2093	500	LØADED UP
481	3248	3229	470	LØADED UP

TABLE V
THE DROP MODEL

CRITICAL WEBER NUMBER = 60

WELL NO	CALCULATED MINIMUM FLOW RATES SURF MCFD	BOTTOM MCFD	TEST FLOW RATE MCFD	FLOW CONDITION
11	927	922	775	NEAR L.U.
21	693	662	417	NEAR L.U.
31	363	419	568	NEAR L.U.
41	786	767	712	NEAR L.U.
51	498	480	442	NEAR L.U.
61	1375	1239	1525	LOADED UP
62	1368	1239	2926	UNLOADED
71	1377	1256	2494	NEAR L.U.
72	1358	1249	3726	UNLOADED
81	2869	2680	2611	LOADED UP
82	2855	2670	3264	NEAR L.U.
83	2848	2667	4095	NEAR L.U.
91	1945	1802	1814	LOADED UP
92	1903	1772	2915	NEAR L.U.
93	1869	1746	2915	UNLOADED
101	1318	1220	1792	LOADED UP
102	1290	1216	2572	UNLOADED
111	1930	1794	2261	LOADED UP
112	1915	1779	2503	NEAR L.U.
113	1872	1754	3351	UNLOADED
121	1297	1223	2069	NEAR L.U.
122	1287	1216	2769	UNLOADED
131	1974	1895	2542	LOADED UP
132	1967	1893	3182	NEAR L.U.
133	1960	1890	3890	UNLOADED
141	1907	1827	2547	LOADED UP
142	1865	1794	3517	UNLOADED
151	2326	2239	3472	LOADED UP
152	2309	2225	4896	NEAR L.U.
153	2295	2208	6946	UNLOADED
161	1113	1051	1116	NEAR L.U.
162	1082	1032	1959	UNLOADED
171	4480	4812	5501	LOADED UP
172	4467	4903	6405	NEAR L.U.
173	4456	5021	7504	UNLOADED
181	3902	3694	3009	LOADED UP
182	3845	3649	3551	NEAR L.U.
183	3800	3615	4150	UNLOADED
191	5851	5803	4441	LOADED UP

78

THE DRØP MØDEL

CRITICAL WEBER NUMBER = 60

WELL NO	CALCULATED MINIMUM FLØW RATES SURF MCFD	BØTTØM MCFD	TEST FLØW RATE MCFD	FLØW CONDITIØN
192	5700	5669	4843	LØADED UP
193	5529	5525	5513	UNLØADED
201	7053	7118	8185	LØADED UP
202	7018	7098	9039	NEAR L.U.
203	6965	7070	9897	UNLØADED
211	7232	7211	6702	LØADED UP
212	7153	7154	8210	NEAR L.U.
213	7084	7105	9289	UNLØADED
221	6636	6633	7109	LØADED UP
222	6610	6646	8406	NEAR L.U.
223	6582	6662	9747	UNLØADED
231	6708	6730	6361	LØADED UP
232	6745	6804	8057	NEAR L.U.
233	6523	6659	9860	UNLØADED
234	6199	6463	11767	UNLØADED
241	4296	4523	4124	LØADED UP
242	4058	4475	4998	NEAR L.U.
243	3805	4562	6423	UNLØADED
251	1474	1574	8672	UNLØADED
252	1673	1655	6654	UNLØADED
253	1745	1694	5136	UNLØADED
254	1787	1719	3917	UNLØADED
261	2106	1921	3376	UNLØADED
262	2060	1913	4830	UNLØADED
263	2028	1906	6221	UNLØADED
264	1973	1895	7792	UNLØADED
271	1012	978	1138	UNLØADED
272	968	941	1712	UNLØADED
273	892	879	2473	UNLØADED
274	816	819	2965	UNLØADED
281	1041	998	1797	UNLØADED
282	1021	994	2502	UNLØADED
283	989	983	3460	UNLØADED
284	955	970	4439	UNLØADED
285	910	960	5656	UNLØADED
291	1446	1334	1596	UNLØADED
292	1399	1296	2423	UNLØADED
293	1272	1215	3598	UNLØADED
294	1091	1120	4410	UNLØADED

THE DROP MODEL

CRITICAL WEBER NUMBER = 60

WELL NO	CALCULATED MINIMUM FLOW RATES SURF MCFD	BOTTOM MCFD	TEST FLOW RATE MCFD	FLOW CONDITION
301	992	948	2939	UNLOADED
302	972	944	4140	UNLOADED
303	916	939	5820	UNLOADED
304	887	936	6871	UNLOADED
311	1069	1007	1943	UNLOADED
312	991	958	2910	UNLOADED
313	897	904	3742	UNLOADED
314	812	865	4485	UNLOADED
331	1608	1522	2688	UNLOADED
332	1578	1514	3585	UNLOADED
333	1539	1504	4380	UNLOADED
334	1545	1538	5270	UNLOADED
341	1876	1710	2700	UNLOADED
342	1793	1644	3176	UNLOADED
343	1732	1609	3925	UNLOADED
344	1658	1565	4619	UNLOADED
351	11286	10511	4242	UNLOADED
352	11205	10464	5050	UNLOADED
353	11060	10397	6111	UNLOADED
354	10889	10294	7571	UNLOADED
361	1409	1342	3322	UNLOADED
362	1386	1329	3809	UNLOADED
363	1357	1307	4634	UNLOADED
364	1305	1275	5422	UNLOADED
371	1811	1701	2873	UNLOADED
372	1782	1695	4288	UNLOADED
373	1737	1694	6077	UNLOADED
374	1682	1697	7992	UNLOADED
381	1263	1187	1540	UNLOADED
382	1272	1183	2439	UNLOADED
383	1287	1176	3436	UNLOADED
384	1258	1169	4471	UNLOADED
391	1220	1132	1550	UNLOADED
392	1185	1107	1804	UNLOADED
393	1119	1058	2385	UNLOADED
394	1018	979	2949	UNLOADED
401	6063	5662	3024	UNLOADED
402	5999	5637	3863	UNLOADED
411	1366	1279	1247	LOADED UP

THE DROP MODEL

CRITICAL WEBER NUMBER = 60

WELL NO	CALCULATED MINIMUM FLOW RATES SURF MCFD	BOTTOM MCFD	TEST FLOW RATE MCFD	FLOW CONDITION
412	1307	1230	1313	LOADED UP
413	1423	1329	1356	LOADED UP
414	1688	1549	1365	LOADED UP
415	1139	1099	1607	LOADED UP
421	6057	5991	5740	NEAR L.U.
422	7043	6951	3890	LOADED UP
423	7357	7256	2780	LOADED UP
424	7563	7456	1638	LOADED UP
441	2597	2633	400	LOADED UP
451	2052	2126	800	LOADED UP
461	7572	7557	4300	LOADED UP
471	2478	2489	500	LOADED UP
481	3862	3841	470	LOADED UP

TABLE VI

WELL NØ	TEST FLOW RATE MCFD	DEPTH ØF WELL FT	WELL HEAD PRES PSIA	WELL HEAD TEMP F	BØT HØLE TEMP F	SURF TENS D/CM	LIQ GRV API	CØND MAKE B/MM	WATER MAKE B/MM	TUBING ID IN	TUBING ØD IN	CASING ID IN	FLØW CØNDITIØN
11	775	6404	725	99	173	20	63.8	6.0	0.	2.441			NEAR L.U.
21	417	6739	400	70	197	60	0.	0.	18.0	1.995			NEAR L.U.
31	568	6529	108	74	151	60	64.3	9.6	12.4	2.041			NEAR L.U.
41	712	6700	540	87	196	60	70.8	10.5	10.5	1.995			NEAR L.U.
51	442	6770	450	90	210	21	61.0	11.3	0.	1.995			NEAR L.U.
61	1525	11200	3607	79	254	20	61.0	37.4	0.	1.995			LØADED
62	2926	11200	3434	82	254	21	61.0	37.4	0.	1.995			UNLØADED
71	2494	11340	3773	85	255	20	58.0	36.8	0.	1.995			NEAR L.U.
72	3726	11340	3660	90	255	20	58.0	36.8	0.	1.995			UNLØADED
81	2611	11416	3340	92	245	20	56.4	130.8	0.	2.992			LØADED
82	3264	11416	3295	93	245	20	56.4	130.8	0.	2.992			NEAR L.U.
83	4095	11416	3280	94	245	20	56.4	130.8	0.	2.992			NEAR L.U.
91	1814	11417	3540	89	254	20	56.4	113.5	0.	2.441			LØADED
92	2915	11417	3340	95	254	20	56.4	113.5	0.	2.441			NEAR L.U.
93	2915	11417	3190	99	254	20	56.4	113.5	0.	2.441			UNLØADED
101	1792	11426	3525	81	245	20	55.0	106.9	0.	1.995			LØADED
102	2572	11426	3472	96	245	20	55.0	106.9	0.	1.995			UNLØADED
111	2261	11355	3338	88	245	20	55.0	117.6	0.	2.441			LØADED
112	2503	11355	3245	88	245	20	55.0	117.6	0.	2.441			NEAR L.U.
113	3351	11355	3092	95	245	20	55.0	117.6	0.	2.441			UNLØADED
121	2069	11390	3556	97	244	20	55.0	104.3	0.	1.995			NEAR L.U.
122	2769	11390	3455	97	244	20	55.0	104.3	0.	1.995			UNLØADED
131	2542	8690	3665	92	194	19	60.0	68.3	0.	2.441			LØADED
132	3182	8690	3644	94	194	19	60.0	68.3	0.	2.441			NEAR L.U.
133	3890	8690	3615	95	194	19	60.0	68.3	0.	2.441			UNLØADED
141	2547	8840	3212	95	198	19	60.0	54.8	0.	2.441			LØADED
142	3517	8840	3025	97	198	19	60.0	54.8	0.	2.441			UNLØADED
151	3472	11850	8215	98	240	19	67.5	10.8	0.	2.441			LØADED
152	4896	11850	7930	100	240	19	67.5	10.8	0.	2.441			NEAR L.U.
153	6946	11850	7405	102	240	19	67.5	10.8	0.	2.441			UNLØADED

WELL NO	TEST FLOW RATE MCFD	DEPTH OF WELL FT	WELL HEAD PRES PSIA	WELL HEAD TEMP F	BOT HOLE TEMP F	SURF TENS D/CM	LIQ GRV API	COND MAKE B/MM	WATER MAKE B/MM	TUBING ID IN	TUBING OD IN	CASING ID IN	FLOW CONDITION
161	1116	6993	2335	107	210	18	65.0	17.9	0.	1.995			NEAR L.U.
162	1959	6993	2225	112	210	18	65.0	17.9	0.	1.995			UNLOADED
171	5501	5723	2182	138	182	15	70.0	2.5	0.		4.500	6.184	LOADED
172	6405	5723	2175	139	182	15	70.0	2.5	0.		4.500	6.184	NEAR L.U.
173	7504	5723	2169	140	182	15	70.0	2.5	0.		4.500	6.184	UNLOADED
181	3009	5513	1590	88	176	21	65.0	13.1	0.	3.958			LOADED
182	3551	5513	1550	89	176	21	65.0	13.1	0.	3.958			NEAR L.U.
183	4150	5513	1520	90	176	21	65.0	13.1	0.	3.958			UNLOADED
191	4441	6180	1245	120	189	16	67.0	10.3	0.		2.875	6.184	LOADED
192	4843	6180	1184	120	189	16	67.0	10.3	0.		2.875	6.184	LOADED
193	5513	6180	1117	120	189	16	67.0	10.3	0.		2.875	6.184	UNLOADED
201	8185	6031	1958	137	186	15	62.5	24.8	0.		2.875	6.184	LOADED
202	9039	6031	1938	137	186	15	62.5	24.8	0.		2.875	6.184	NEAR L.U.
203	9897	6031	1913	138	186	15	62.5	24.8	0.		2.875	6.184	UNLOADED
211	6702	5962	2040	130	185	15	65.0	31.8	0.		2.875	6.184	LOADED
212	8210	5962	1993	130	185	15	65.0	31.8	0.		2.875	6.184	NEAR L.U.
213	9289	5962	1953	130	185	15	65.0	31.8	0.		2.875	6.184	UNLOADED
221	7109	5906	2284	128	184	15	67.5	15.1	0.		3.500	6.184	LOADED
222	8406	5906	2271	129	184	15	67.5	15.1	0.		3.500	6.184	NEAR L.U.
223	9747	5906	2256	130	184	15	67.5	15.1	0.		3.500	6.184	UNLOADED
231	6361	5934	2352	134	184	15	70.0	3.7	0.		3.500	6.184	LOADED
232	8057	5934	2388	135	184	15	70.0	3.7	0.		3.500	6.184	NEAR L.U.
233	9860	5934	2223	136	184	15	70.0	3.7	0.		3.500	6.184	UNLOADED
234	11767	5934	2003	138	184	15	70.0	3.7	0.		3.500	6.184	UNLOADED
241	4124	6850	2042	138	201	15	65.0	26.7	0.		4.500	6.184	LOADED
242	4998	6850	1818	139	201	15	65.0	26.7	0.		4.500	6.184	NEAR L.U.
243	6423	6850	1600	140	201	15	65.0	26.7	0.		4.500	6.184	UNLOADED
251	8672	7346	1935	104	210	55	52.7	27.8	0.4	1.995			UNLOADED
252	6654	7346	2421	108	210	55	52.7	27.8	0.4	1.995			UNLOADED
253	5136	7346	2705	112	210	55	52.7	27.8	0.4	1.995			UNLOADED

WELL NO	TEST FLOW RATE MCFD	DEPTH OF WELL FT	WELL HEAD PRES PSIA	WELL HEAD TEMP F	BOT HOLE TEMP F	SURF TENS D/CM	LIQ GRV API	COND MAKE B/MM	WATER MAKE B/MM	TUBING ID IN	TUBING OD IN	CASING ID IN	FLOW CONDITION
254	3917	7346	2884	114	210	55	52.7	27.8	0.4	1.995			UNLOADED
261	3376	8963	5056	109	271	55	43.9	7.5	1.4	1.995			UNLOADED
262	4830	8963	4931	126	271	55	43.9	7.5	1.4	1.995			UNLOADED
263	6221	8963	4786	134	271	55	43.9	7.5	1.4	1.995			UNLOADED
264	7792	8963	4575	149	271	55	43.9	7.5	1.4	1.995			UNLOADED
271	1138	5294	1902	100	170	20	71.0	30.9	0.	1.995			UNLOADED
272	1712	5294	1737	100	170	20	71.0	0.9	0.	1.995			UNLOADED
273	2473	5294	1480	100	170	20	71.0	0.9	0.	1.995			UNLOADED
274	2965	5294	1246	98	170	20	71.0	0.9	0.	1.995			UNLOADED
281	1797	5234	1895	87	162	20	71.7	54.1	0.	1.995			UNLOADED
282	2502	5234	1861	93	162	20	71.7	54.1	0.	1.995			UNLOADED
283	3460	5234	1784	100	162	20	71.7	54.1	0.	1.995			UNLOADED
284	4439	5234	1680	103	162	20	71.7	54.1	0.	1.995			UNLOADED
285	5656	5234	1551	108	162	20	71.7	540.1	0.	1.995			UNLOADED
291	1596	7639	2814	87	209	55	53.5	3.3	1.0	1.750			UNLOADED
292	2423	7639	2582	85	209	55	53.5	3.3	1.0	1.750			UNLOADED
293	3598	7639	2104	86	209	55	53.5	3.3	1.0	1.750			UNLOADED
294	4410	7639	1575	90	209	55	53.5	3.3	1.0	1.750			UNLOADED
301	2939	7475	2783	100	203	20	52.4	3.4	0.	1.750			UNLOADED
302	4140	7475	2655	101	203	20	52.4	3.4	0.	1.750			UNLOADED
303	5820	7475	2406	113	203	20	52.4	3.4	0.	1.750			UNLOADED
304	6871	7475	2205	108	203	20	52.4	3.4	0.	1.750			UNLOADED
311	1943	7546	2574	97	205	20	52.2	4.1	0.6	1.750			UNLOADED
312	2910	7546	2224	103	205	20	52.2	4.1	0.6	1.750			UNLOADED
313	3742	7546	1839	107	205	20	52.2	4.1	0.6	1.750			UNLOADED
314	4485	7546	1509	106	205	20	52.2	4.1	0.6	1.750			UNLOADED
331	2688	6965	2409	120	228	55	56.5	26.5	1.0	1.995			UNLOADED
332	3585	6965	2340	124	228	55	56.5	26.5	1.0	1.995			UNLOADED
333	4380	6965	2259	130	228	55	56.5	26.5	1.0	1.995			UNLOADED
334	5270	6965	2155	134	228	55	56.5	26.5	1.0	1.995			UNLOADED

WELL NO	TEST FLOW RATE MCFD	DEPTH OF WELL FT	WELL HEAD PRES PSIA	WELL HEAD TEMP F	BOT HOLE TEMP F	SURF TENS D/CM	LIQ GRV API	COND MAKE B/MM	WATER MAKE B/MM	TUBING ID IN	TUBING OD IN	CASING ID IN	FLOW CONDITION
341	2700	8304	2974	96	241	55	52.1	9.1	0.3	1.995			UNLOADED
342	3176	8304	2677	98	241	55	52.1	9.1	0.3	1.995			UNLOADED
343	3925	8304	2499	101	241	55	52.1	9.1	0.3	1.995			UNLOADED
344	4619	8304	2284	103	241	55	52.1	9.1	0.3	1.995			UNLOADED
351	4242	7508	2837	100	216	20	55.2	6.5	0.		2.375	6.366	UNLOADED
352	5050	7508	2805	102	216	20	55.2	6.5	0.		2.375	6.366	UNLOADED
353	6111	7508	2761	107	216	20	55.2	6.5	0.		2.375	6.366	UNLOADED
354	7571	7508	2693	111	216	20	55.2	6.5	0.		2.375	6.366	UNLOADED
361	3322	8819	3734	100	212	20	50.8	4.0	0.	1.995			UNLOADED
362	3809	8819	3601	104	212	20	50.8	4.0	0.	1.995			UNLOADED
363	4634	8819	3382	105	212	20	50.8	4.0	0.	1.995			UNLOADED
364	5422	8819	3082	110	212	20	50.8	4.0	0.	1.995			UNLOADED
371	2873	7565	2715	99	211	55	53.9	8.5	1.2	1.995			UNLOADED
372	4288	7565	2633	101	211	55	53.9	8.5	1.2	1.995			UNLOADED
373	6077	7565	2515	105	211	55	53.9	8.5	1.2	1.995			UNLOADED
374	7992	7565	2350	106	211	55	53.9	8.5	1.2	1.995			UNLOADED
381	1540	7753	2750	105	217	20	52.6	5.5	0.	1.995			UNLOADED
382	2439	7753	2700	95	217	20	52.6	5.5	0.	1.995			UNLOADED
383	3436	7753	2611	78	217	20	52.6	5.5	0.	1.995			UNLOADED
384	4471	7753	2527	84	217	20	52.6	5.5	0.	1.995			UNLOADED
391	1550	8162	2556	92	217	20	56.7	7.7	0.	1.995			UNLOADED
392	1804	8162	2415	96	217	20	56.7	7.7	0.	1.995			UNLOADED
393	2385	8162	2149	100	217	20	56.7	7.7	0.	1.995			UNLOADED
394	2949	8162	1765	100	217	20	56.7	7.7	0.	1.995			UNLOADED
401	3024	7810	2862	96	214	20	52.2	5.0	0.		2.375	4.974	UNLOADED
402	3863	7810	2823	100	214	20	52.2	5.0	0.		2.375	4.974	UNLOADED
411	1247	7531	760	83	230	55	54.9	46.1	54.1	2.441			LOADED
412	1313	7531	704	82	230	55	54.9	31.6	40.8	2.441			LOADED
413	1356	7531	822	83	230	55	54.9	26.7	26.3	2.441			LOADED
414	1365	7531	1102	83	230	55	54.9	26.1	23.8	2.441			LOADED

WELL NO	TEST FLOW RATE MCFD	DEPTH OF WELL FT	WELL HEAD PRES PSIA	WELL HEAD TEMP F	BOT HOLE TEMP F	SURF TENS D/CM	LIQ GRV API	COND MAKE B/MM	WATER MAKE B/MM	TUBING ID IN	TUBING OD IN	CASING ID IN	FLOW CONDITION
415	1607	7531	552	83	230	55	54.9	25.1	22.3	2.441			LOADED
421	5740	3278	315	85	130	20	50.0	10.0	0.	7.386			NEAR L.U.
422	3890	3278	422	85	130	20	50.0	10.0	0.	7.386			LOADED
423	2780	3278	459	85	130	20	50.0	10.0	0.	7.386			LOADED
424	1638	3278	484	85	130	20	50.0	10.0	0.	7.386			LOADED
441	400	5080	500	90	130	20	50.0	14.0	0.		2.375	4.974	LOADED
451	800	7200	500	90	175	55	0.	0.	5.0		2.375	4.052	LOADED
461	4300	6776	660	90	165	55	0.	0.	3.5		2.375	6.276	LOADED
471	500	3077	280	90	130	60	0.	0.	28.0		2.375	4.974	LOADED
481	470	2250	210	90	125	60	0.	0.	24.0		2.375	6.276	LOADED
LAB	123	16	19.1	72		60			17.5	1.875			UNLOADED
LAB	109	16	18.9	72		60			19.8	1.875			UNLOADED
LAB	84	16	18.5	72		60			25.6	1.875			UNLOADED
LAB	65	16	18.2	72		60			33.2	1.875			LOADED
LAB	122	16	19.2	72		60			6.8	1.875			UNLOADED
LAB	105	16	18.7	72		60			7.9	1.875			UNLOADED
LAB	81	16	18.4	72		60			10.3	1.875			UNLOADED
LAB	58	16	18.0	72		60			14.3	1.875			LOADED

APPENDIX E

Computer Programs

Nomenclature Used in Film Model Program.

Input Variables

L	=	Well test sequence number	
P	=	Wellhead pressure	psia
XL	=	Depth of Well	ft
TS	=	Surface flowing temperature	°F
TB	=	Bottom-hole flowing temperature	°F
ST	=	Surface tension of the liquid	dy/cm
GG	=	Gravity of the gas (Air = 1.00)	
GL	=	Gravity if the liquid	°API
TID	=	Inside diameter of the tubing	in
RW	=	Rate of water production	bbl/mmcf
RC	=	Rate of condensate production	bbl/mmcf
M	=	Logical Integer = 1 if production is through tubing	
		= 0 if production is through annulus	
K	=	Logical Integer = 1 if well is unloaded	
		= 0 if well is near loadup	
		=-1 if well is loaded up	
TOD	=	Tubing outside diameter	in
CID	=	Casing inside diameter	in

Calculated variables

XMUL	= Liquid phase viscosity	lbm/ft-sec
XMUG	= Gas phase viscosity	lbm/ft-sec
TAVE	= Average flowing temperature	°R
RHOG(1)	= Gas phase density @ surface conditions	lbm/ft^3
RHOG(2)	= Gas phase density @ bottom-hole conditions	lbm/ft^3
RHOL	= Liquid phase density	lbm/ft^3
RENG	= Reynolds modulus for gas phase	
RENL	= Reynolds modulus for liquid phase	
FG	= Fanning friction factor for gas phase	
FL	= Fanning friction factor for liquid phase	
DPDLG	= Gas phase pressure drop	
DPDLL	= Liquid phase pressure drop	
DPDL2	= Two-phase pressure drop	
TAUO	= Shear stress at the wall	lbf/ft^2
USTAR	= Friction velocity	ft/sec
BETA	= Dimensionless interfacial shear	
ETA	= Dimensionless film thickness	
SIGETA	= $\frac{\sigma^3}{\eta}$	
YPMAXA	= y_m^+	
PHI	= $\frac{y_m^+ - 60}{22}$	
YPLUSS	= y^+	
UPLUS	= u^+	

Sub programs called

ZFACT (P,T,G) = The deviation from the perfect gas laws		
P	= Pressure	psia
T	= Temperature	°R
G	= Gravity of gas (Air = 1.000)	
PSF (P,G,T,D,XL,Q) = The bottom-hole flowing pressure		
T	= Average flowing temperature	°R
D	= Diameter of tubing	in
XL	= Depth of well	ft
Q	= Flow rate of gas	mmcf/d
SIMPSN(X1,X2,N) = Numerical integration routine		
X1	= Interval of finite difference	
X2	= Values of function (Array of length N)	
N	= Number of points in array (N-1 intervals)	

```
      DIMENSIØN U(5),UPLUS(5),FY(5),FUY(5),YPLUSS(37),UPLUU(37),
     1YS(37),US(37)
      DIMENSIØN RHØG(2),LQX(2)
      DATA YPLUSS/1.,2.,3.,4.,5.,6.,7.,8.,9.,10.,20.,30.,40.,50.,60.,70.
     1,80.,90.,100.,200.,300.,400.,500.,600.,700.,800.,900.,1000.,2000.,
     23000.,4000.,5000.,6000.,7000.,8000.,9000.,10000./
    4 JJJ = 1
      WRITE(6,6999)
      WRITE (6,7001)
 6999 FØRMAT(1H1///31X,14HTHE FILM MØDEL//)
 7001 FØRMAT(1H    ,17X,4HWELL,2X,10HCALCULATED,13H  CALCULATED ,4HTEST,
     17X,4HFLØW/19X,2HNØ,6X,4HFLØW,8X,4HFLØW,4X,4HFLØW,5X,9HCØNDITIØN/27
     2X,4HRATE,8X,4HFLØW,4X,4HRATE/25X,7HSURFACE,6X,6HBØTTØM///)
    5 READ(5,10) N,P,Q,XL,TS,TB,ST,GG,GL,TID,RW,RC,M,K,TØD,CID
   10 FØRMAT (I5,6F5.0,F5.3,F5.1,F5.3,2F5.1,2I2,2F5.3)
      IF ( RW .NE. 0. .AND. RC .NE. 0. ) GØ TØ 5
      IF (N.GT.330) TB = TB/10.
      TSU = TS + 460.
      TBH = TB + 460.
      PI = 3.14159
      SGL = 141.5/(131.5+GL)
      IF(RW .NE.0.) SGL = 1.08
      TAVE = (TSU + TBH)/2.
      D = TID
      TID = TID/12.
      XMUL = .000672 * .300
      VISC = .015
      XMUG = VISC*.000672
      RHØL = 62.4*SGL
      QØ = Q/ 1000.
      LQØ = Q
      PBH = PSF(P,GG,TAVE,D,XL,QØ)
      RHØG(1) = P*29.*GG/(ZFACT(P,TSU,GG)*10.73*TSU)
      RHØG(2) = PBH*29.*GG/(ZFACT(PBH,TBH,GG)*10.73*TBH)
      RRL = RC
      IF (RW.NE.0.0) RRL = RW
      DØ 200 III=1,2
      QL = QØ*RRL*5.615*RHØL/86400.
      I = 1
      QX = 10.
      DQX = 5.
   20 QG = QX*29.*GG*1.E+6*(1./86400.)/379.
      RENG = 4.*QG/(PI*TID*XMUG)
      RENL = 4.*QL/(PI*TID*XMUL)
      FG = .0014+(.125/(RENG**.32))
      FL = .0014+(.125/(RENL**.32))
      ZZ = 32./(PI**2*32.2*TID**5)
      DPDLG = QG**2*ZZ*FG/RHØG(III)
      DPDLL = QL**2*ZZ*FL/RHØL
      DPDL2 = 10.89*DPDLG*(DPDLL/DPDLG)**.22
      TAUØ = TID/4.*DPDL2*.01
      USTAR = SQRT (TAUØ*32.2/RHØL)
      BETA=DPDL2*RHØL**(2./3.)*32.2**(1./3.)/(RHØL*XMUL**(2./3.))*TID/4.
      ETA = SQRT((BETA/4.67)**3)
      IF (ETA .GT. 10000. ) GØ TØ 300
```

```
      [illegible]
      [illegible]
      PHI = (YPMAXA-60.)/22.
      N = 5
      XWF = 0.
      UPLUS(N) = 0.
      FY(N) = 0.
      II = 1
      YPL = 0.
      FUY(N) = 0.
  120 YPH = YPLUSS(II)
      IF (YPLUSS(II).GT.ETA) GØ TØ 122
      DYP = (YPH-YPL)/4.
      GØ TØ 123
  122 DYP = (ETA - YPL)/4.
      YPH = ETA
  123 DDYP = DYP/4.
      FUY(1) = FUY(N)
      IU = 1
      UPLUS(IU) = UPLUS(N)
      U(IU) = UPLUS(IU) * USTAR
      YPLU = YPL
  124 FY(1) = FY(N)
      YPHU = YPLU + DYP
      YPLUS = YPHU
      J = 5
  125 YPDYM = YPLUS/YPMAXA
      EXPCHX = PHI*YPDYM
      ATERM = 0.
      IF (EXPCHX.LT.80.) ATERM =(1./EXP(EXPCHX))
      ACHECK = (1.-ATERM)**2
      FY(J)=2.*(1.+YPLUS*SIGETA)/(1.+SQRT(1.+4.*.1296*YPLUS**2*ACHECK**2
     1*(1.+YPLUS*SIGETA)))
      J = J-1
      IF (J.LT.2 ) GØ TØ 126
      YPLUS = YPLUS +DDYP
      GØ TØ 125
  126 IU = IU + 1
      UPLUS(IU) = UPLUS(IU-1)+SIMPSN(DDYP,FY(1),N)
      IF (IU.GE.N) GØ TØ 127
      YPLU = YPHU
      GØ TØ 124
  127 J = 5
      YPLUS = YPH
  128 FUY(J) = UPLUS(J)
      U(J) = UPLUS(J) * USTAR
      Y = YPH * XMUL * USTAR / RHØL
      J = J-1
      IF (J.LT.2) GØ TØ 129
      GØ TØ 128
  129 WFINC = SIMPSN(DYP,FUY(1),N)
      XWF = XWF + WFINC
  790 IF(ETA.LE.YPLUSS(II).AND.ETA.GT.YPLUSS(II-1)) GØ TØ 130
      II = II +1
      IF ( II .GT. 37) GØ TØ 5
      YPL = YPH
```

```
      GO TO 120
  300 WRITE (6,555)
  555 FØRMAT (1HO,13HETA TØØ LARGE)
      GØ TØ 174
  130 WF = PI *TID*XMUL * XWF
C  USE HALF INTERVAL CØNVERGENCE
      IF(QL .LT. WF) GØ TØ 175
  174 QX = QX + DQX
      DQX = DQX/ 2.
      I = I + 1
      IF ( I .GT. 16 ) GØ TØ 185
      GØ TØ 20
  175 QX = QX - DQX
      DQX = DQX/ 2.
      I = I + 1
      IF ( I .GT. 16 ) GØ TØ 185
      GØ TØ 20
  185 LQX(III) = QX * 1000.
  200 CØNTINUE
      IF(M) 190,191,192
  190 WRITE(6,7000) L,LQX,LQØ
      GØ TØ 220
  191 WRITE(6,7002) L,LQX,LQØ
      GØ TØ 220
  192 WRITE(6,7003) L,LQX,LQØ
  220 JJJ = JJJ + 1
      IF(JJJ.GT. 47) GØ TØ 4
      GØ TØ 5
 7000 FØRMAT(1H ,I20,3I10,5X,9HLØADED UP)
 7002 FØRMAT(1H ,I20,3I10,5X,9HNEAR L.U.)
 7003 FØRMAT(1H ,I20,3I10,5X,8HUNLØADED)
      END
```

```
      FUNCTION PSF(P,G,T,D,XL,Q)
      X = D**5.23
      BB = 18.768*G*(XL/1000.)/T
      AI = 14.97*Q**2*T**2/X
      PST = P+ 18.77*G*(XL/1000.)*P/T
      I = 1
   10 PA = (PST+P)/2.
      Z =ZFACT (PA,T,G)
      IF (Z.EQ. 0.0) GO TO 50
      B = EXP(2.*BB/Z)
      A = AI*Z**2.
      PS2F = P**2*B+A*(B-1.)
      PSFC = SQRT (PS2F )
      IF ( ABS ((PSFC-PST)/PSFC*100.).LE.0.1) GO TO 40
   30 PST = PSFC
      I = I + 1
      GO TO 10
   40 PSF = PSFC




      GO TO 52
   50 PSF = 0.0
   52 CONTINUE
      RETURN
      END
```

```
      FUNCTION ZFACT (P,T,G)
      PC=699.3023-46.5516*G
      TC=313.7255*G+169.902
      E1=P/PC
      E2=T/TC
      I=1
      TEMP=0.
      IF (E1 .LT. 9.5) GO TO 30
20    Z=1.1
      GO TO 50
30    Z=1.0
35    E3=Z*(E2/E1)
      E4=.05/(E3*E2**3)
      E5=.4758*(1.-.1127/E3)
      E6=.18764*(1.-.03833/E3)
      Z=(1.-E4)/E3*(E3+E6)-E5/(E2*E3)
      IF (ABS(Z-TEMP)/Z*100..LE..1) GO TO 38
      IF (I.LE.100) GO TO 37
36    Z=0.
      GO TO 60
37    TEMP=Z
      I=I+1
      GO TO 35
38    IF (P.GE.1000.) GO TO 40
39    Z=Z-.0072
      GO TO 60
40    IF (Z.GE.1.) GO TO 42
41    Z=Z-.015
      GO TO 60
42    Z=Z+.01
      GO TO 60
50    E7=E2**3
      E8=E1/E2
      E9=(.18764-.05/E7-.4758/E2)*E8
      E10=(.053623/E2-.0071922-.009382/E7)*(E8**2)
      E11=(3.5961E-4/E7)*(E8**3)
51    I=I+1
      IF (I.LE.100) GO TO 53
52    Z=0.
      GO TO 60
53    EB=Z**4-Z**3-E9*Z**2-E10*Z-E11
      IF (EB.GE.0.) GO TO 55
54    Z=Z-EB/2.
      GO TO 51
55    IF (EB.LE..2) GO TO 59
      Z=Z-.01
      GO TO 51
59    Z=Z+.031
60    ZFACT=Z
      RETURN
      END
```

```
      FUNCTIØN SIMPSN(X1,X2,N)
      DIMENSIØN X2(N)
      SUM = X2(1)-X2(N)
      NN = N/2
      DØ 10 I = 1,NN
   10 SUM = SUM +4.*X2(2*I)+2.*X2(2*I+1)
      SIMPSN = X1*SUM/3.
      RETURN
      END
```

APPENDIX F

Nomenclature

A	= Flow area	ft^2
A_p	= Projected area of particle	ft^2
b	$= \sqrt[3]{\frac{\eta^2 \mu_L^2}{\rho_L^2}}$	
C	= Constant in radial gas flow equation	
C	= Constant in Wallis flooding point equation	
C_d	= Drag coefficient	
D	= Diameter of tube	ft
D_I	= Diameter of tube	inches
d	= Droplet diameter	ft
d_m	= Maximum droplet diameter	ft^2
$\frac{du}{dy}$	= Velocity gradient of moving liquid	
$\frac{du^+}{dy^+}$	= Dimensionless velocity gradient	
e	= Natural logarithm base = 2.718	
F	$= \frac{\frac{\Delta P}{\Delta x} - \rho_G \frac{g_L}{g_c}}{\rho_L \frac{g_L}{g_c}}$	
F_d	= Drag force of falling particle	lbsf
F_G	= Gravitational force	lbsf
$F\uparrow$	= Upward acting force	lbsf
$F_o\downarrow$	= Wall friction forces	lbsf
G	= Gravity of gas (Air - 1.00)	

g_L	= Local acceleration of gravity	$\frac{ft}{sec^2}$
g_c	= Gravitational constant = 32.17	$\frac{ft\ lbm}{sec^2\ lbf}$
k	= Universal constant = .36	
M	= Molecular weight	$\frac{lbsm}{mole}$
m	= Film thickness	ft
N_{Re}	= Drop Reynolds Number = $\frac{\rho_G d u_T}{\mu_G}$	
N_{ReG}	= Reynolds modulus of gas phase	
N_{ReL}	= Reynolds modulus of liquid phase	
N_{We}	= Weber number	
P	= Pressure	psia
P_F	= Formation pressure	psia
P_S	= Sandface (flowing) pressure	psia
Q	= Gas flow rate	mcf/day
Q_J	= Gas flow rate in Jones' equation	mmcf/day
Q_{MM}	= Gas flow rate	mmcf/day
R	= Universal gas constant = 10.73	
R_L	= Liquid volume fraction	
R_G	= Gas volume fraction	
Su	= Parameter in Hughes and Gilliland Correlation	
T	= Temperature	°R
u	= Velocity	$\frac{ft}{sec}$
u*	= Friction velocity	$\frac{ft}{sec}$
u^+	= Dimensionless velocity parameter	

u_L	= Average velocity of liquid phase	ft/sec
u_G	= Average velocity of gas phase	ft/sec
V_G	= Dimensionless superficial gas velocity	
V_L	= Dimensionless superficial liquid velocity	
V_{SG}	= Superficial gas velocity	ft/sec
V_{SL}	= Superficial liquid velocity	ft/sec
W_G	= Gas mass flow rate	$\frac{lbm}{sec}$
W_L	= Liquid mass flow rate	$\frac{lbm}{sec}$
X	= Ratio of gravity to interfacial shear force	
X_H	= Parameter in Hughmark Holdup Correlation	
x	= vertical distance (positive upward)	ft
y	= Horizontal distance from wall of tube	ft
y^+	= Dimensionless distance from wall of tube	
y_m^+	= Dimensionless distance parameters evaluated at the center of the tube	
Z	= Deviations from perfect gas law	

Greek Letter Notations

β	= Dimensionless interfacial shear	
$\frac{\Delta P}{\Delta x_G}$	= Gas phase pressure drop	$\frac{lbf/ft^2}{ft}$
$\frac{\Delta P}{\Delta x_L}$	= Liquid phase pressure drop	$\frac{lbf/ft^2}{ft}$

$\frac{\Delta p}{\Delta X_{TP}}$	= Two-phase pressure drop	$\frac{lbf/ft^2}{ft}$
η	= Dimensionless film thickness	
μ_G	= Gas viscosity (absolute)	$\frac{lbm}{ft\ sec}$
μ_L	= Liquid viscosity (absolute)	$\frac{lbm}{ft\ sec}$
ν	= Kinematic liquid viscosity = $\frac{\mu_L}{\rho_L}$	
ξ	= Eddy viscosity	
π	= 3.14159---	
ρ_L	= Liquid phase density	$\frac{lbm}{ft^3}$
ρ_G	= Gas phase density	$\frac{lbm}{ft^3}$
σ	= $\frac{m}{b}$	
σ_i	= Interfacial tension	$\frac{lbf}{ft}$
σ	= Interfacial tension	$\frac{dynes}{cm}$
τ	= Shear stress	$\frac{lbf}{ft^2}$
τ_i	= Interfacial shear stress	$\frac{lbf}{ft^2}$
τ_o	= Shear stress at the wall of a tube	$\frac{lbf}{ft^2}$
ϕ	= $\frac{v_m^+ - 60}{22}$	
Φ_G	= Parameter in Martinelli Correlation	
X	= Parameter in Martinelli Correlation	